DEGREE PROJECT

Energy neutral user equipment

Tom Brander

Computer Science and Engineering, master's level
2022

Luleå University of Technology
Department of Computer Science, Electrical and Space Engineering

Energy Neutral User Equipment

Tom Brander (tombra-7)

March 2022

Abstract

This thesis investigates if a small vibration energy harvester and/or a photovoltaic panel mounted on a shopping cart can harvest enough energy to power an internet-of-things device to acquire GPS position and transmit the location over a low power wide area network such as NB-IoT or LTE-M. In such a case, how often can we transmit and acquire position?

A demonstrator was built to measure the time spent harvesting energy before the device could acquire GPS position and transmit. In the best conditions the solar panel could produce upwards of 90 mW, resulting in the device being able to transmit continuously. In the best case, the vibration energy harvester produced around 16 mW, resulting in the device transmitting every 23 seconds. In the worst case, or in other words when there are no movement of the shopping cart or no light available for the photovoltaic panel, it will not be able to harvest any power and therefore never be able to gather GPS position and transmit.

Acknowledgement

I would like to thank everyone who have helped me during this project. Special thanks to both my supervisors, Per Lindgren at Luleå University of Technology and Per Bjuréus at Ericsson for guiding me in a theoretical and practical level. Lastly, thanks to Tomás Henriques who designed the power management board for the project.

Stockholm November 2022
Tom Brander

Abbreviations

3GPP - 3rd Generation Partnership Project
Cat M1 - Category M1
Cat NB1 - Category NB1
A-GNSS - Assisted Global Navigation Satelite System
GNSS - Global Navigation Satelite System
GPS - Global Positioning System
LTE-M - Long Term Evolution - Machine Type Communication
NB-IoT - Narrowband Internet of Things
SiP - System-in-package
SoC - System-on-Chip
UE - User Equipment
IoT - Internet of Things
LPWAN - Low power wide area network

Contents

1 Introduction **1**
- 1.1 Background . . . 1
- 1.2 Motivation . . . 1
- 1.3 Problem definition . . . 2
- 1.4 Sustainability . . . 2
- 1.5 Delimitation . . . 2

2 Related work **3**
- 2.1 Energy harvesters . . . 3
  - 2.1.1 Kinetic energy harvester . . . 3
  - 2.1.2 Photovoltaic energy harvester . . . 5
  - 2.1.3 Heat energy harvesting . . . 6
  - 2.1.4 Radio frequency energy harvesting . . . 8
  - 2.1.5 Electromagnetic induction . . . 10
  - 2.1.6 Summary of harvesters . . . 11
- 2.2 Energy storage . . . 12
  - 2.2.1 Energy gravimetric density . . . 12
  - 2.2.2 Capacity retention . . . 13
  - 2.2.3 Materials . . . 13
- 2.3 Low power communications . . . 14
  - 2.3.1 Infrastructure and coverage . . . 14
  - 2.3.2 Data throughput . . . 16
  - 2.3.3 Energy management . . . 16
- 2.4 Network communication protocol . . . 19
  - 2.4.1 User datagram protocol (UDP) . . . 19
  - 2.4.2 Transmission control protocol (TCP) . . . 20
  - 2.4.3 Constraint application protocol (CoAP) . . . 21
  - 2.4.4 Message queuing telemetry transport (MQTT) . . . 22
- 2.5 Global navigation satellite system (GNSS) . . . 22
  - 2.5.1 Carrier-to-noise density (CN0) . . . 23

3 Methodology **24**
- 3.1 Current measurement . . . 24
- 3.2 Harvesters . . . 25
- 3.3 Networks . . . 27
- 3.4 Mounting bracket . . . 29

4 Current measurements **31**
- 4.1 Cat NB1 - transmission (UDP) . . . 31
- 4.2 Cat NB1 - transmission (UDP) using release assistance indication 32
- 4.3 Cat NB1 - transmission (TCP) . . . 32
- 4.4 Cat NB1 - transmission (TCP) using release assistance indication 33
- 4.5 Cat NB1 - idle mode Discontinuous Reception (iDRX) . . . 34
- 4.6 Cat NB1 - PSM . . . 34

4.7 Cat M1 - transmission (UDP) . . . 35
4.8 Cat M1 - transmission (TCP) . . . 35
4.9 Cat M1 - idle mode Discontinuous Reception (iDRX) . . . 36
4.10 Cat M1 - PSM . . . 36
4.11 GNSS . . . 37

5 PMM design **38**

6 Theory **40**
6.1 Vibration energy harvester characteristics . . . 40
6.2 Shopping cart vibrations characteristics . . . 40
6.3 Harvester output . . . 42
6.3.1 Vibration energy harvester . . . 42
6.3.2 Photovoltaic panel . . . 43
6.4 Theoretical model of GNSS fix and LPWAN transmission interval 45

7 Technical choices **47**

8 Software Implementation **48**
8.1 User equipment . . . 48
8.2 Amazon web services - AWS . . . 50
8.2.1 TCP and UDP socket listeners . . . 51
8.2.2 MongoDB . . . 51
8.2.3 Restful API . . . 51
8.2.4 Frontend . . . 52

9 Evaluation **53**
9.1 Theoretical intervals with different average charging current . . . 53
9.2 Actual intervals . . . 54
9.2.1 Vibration energy harvester on parking lot . . . 55
9.2.2 Vibration energy harvester on textured bike lane . . . 57
9.2.3 Photovoltaic panel during clear skies . . . 58
9.2.4 Photovoltaic panel during cloudy skies . . . 60
9.2.5 Summary of actual intervals . . . 61

10 Discussion **62**

11 Conclusion **64**
11.1 Future work . . . 64

1 Introduction

1.1 Background

Since the start of the internet the amount of connected devices has increased exponentially. With the invention of wireless networks such as WiFi networks and cellular networks, devices such as Internet of things (IoT) have become more mobile and able to be implemented in both rural and urban environments.

Devices, micro controllers and tiny sensors are continuously getting smaller, more powerful and more power efficient. Sensors are continuously developing, getting easily obtainable and available, being used in various areas such as measuring air humidity and monitoring 'oil in water'. By making these devices completely wireless with a wireless network connection, and by the use of some sort of energy storage, great benefits for implementation will occur.

IoT devices most often use a lithium ion battery as energy storage. With more devices being implemented every year together with the fact that most lithium ion batteries has a lifetime of about 3-5 years, the environmental and financial impact of changing or replacing these batteries increases accordingly.

In mobile IoT devices development, being able to communicate both wirelessly and power efficiently are two of the most important areas in development of mobile IoT devices. Today there are a lot of options for low power communications such as LoRaWAN, Sigfox, Bluetooth low energy, WiFi, LTE-M and NB-IoT. These network options all have their pros and cons depending on the deployment circumstances of the network.

Nordic semiconductor is a company that specializes in low-power wireless IoT devices. The nrf9160dk (devkit) is built around the nrf9160 system-in-package (SiP) which incorporates an arm cortex m33 application processor and have an integrated modem supporting low power area wide area network (LPWAN) such as LTE-M, narrow band-IoT (NB-IoT) and GNSS. It provides a programmer multiple user programmable buttons, LEDs and switches and many general purpose input/output pins (GPIO) . The thingy91 is also based upon the nrf9160 SiP but compared to the nrf9160dk it provides user programmable peripherals. The thingy91 is powered by a lithium ion battery, have more sensors such as accelerometers and environmental sensors. The thingy91 is also more power efficient since it does not have to power a programmer.

1.2 Motivation

Mobile IoT devices today usually runs on some sort of lithium ion batteries due to their high energy density. These batteries will eventually either have to be charged or replaced because of a bad capacity retention or self discharge. Using a super capacitor which is continuously charged by an energy harvester can last

much longer. This along with using a 3GPP standard wide area network such as LTE-M results in an long lived IoT device that could be implemented without proprietary network solutions in both rural and urban areas.

1.3 Problem definition

It is possible to harvest enough energy using a small energy harvester mounted on a shopping cart to power a thingy91 to get a geographical position and send it over a low power wide area network? Furthermore, how often is it possible to get geographical position and transmit over low power wide area networks using harvested energy? The harvested energy should not be acquired from a dedicated energy source but should instead harvest energy that otherwise would be wasted.

To address these questions, a prototype will be built on a shopping cart to demonstrate this problem. The prototype will have a screen showing the voltage of the energy storage and a backend visualizing the geographical position sent.

1.4 Sustainability

Though producing IoT devices are never environmentally friendly, discarding a lithium ion battery in IoT devices could get IoT devices to become more sustainable. IoT devices without lithium ion batteries would result in less water being wasted in the excavating of lithium, there would be less non-recycled lithium waste and decrease the amount of leaked chemicals from the lithium mines.[27]

1.5 Delimitation

Due to time constraints and Ericsson prioritisation of this project some areas were not investigated during the development of this prototype:

- Other network solutions, such as LoRaWAN, Sigbee, WiFi or Bluetooth to see if it is less power consuming than the NB-IoT and LTE-M.
- Other positioning solutions, such as RSSI indoor location or LORAN.
- Using a piezo electric vibration energy harvester, piezo electric vibration harvesters have a much wider response frequencies compared to electro magnetic vibration harvesters.
- Rust implementation of the application, Rust is continuously getting popularity in embedded systems development since it can guarantee both high performance and security.

One other consideration that was discarded which would be very important in building a real product is the cost of different components, harvesters, microcontrollers and capacitors.

2 Related work

2.1 Energy harvesters

Energy harvesters are small devices that harvest power from its surroundings. The energy often comes from kinetic energy, photovoltaic/light energy, heat energy, radio energy or electromagnetic induction. The amount of power delivered by these harvesters is usually very small and therefore used for low powered devices or sensors.[12]

2.1.1 Kinetic energy harvester

Kinetic energy harvester generates electric energy from vibrations of the harvester itself. Kinetic energy harvesters are therefore often called vibration energy harvesters or VEH. They are divided into three different groups based on their working principle:

- Electromagnetic harvesters
- Piezoelectric harvesters
- Electrostatic harvesters

Electromagnetic

Electromagnetic are the most common type of kinetic energy harvesting because of its price per output compared to the other groups of harvesters. Electromagnetic harvesters uses a magnet that oscillates within a wire coil. The movement of the magnet induces an altering current in the coil, see Figure 1. The vibration frequency must correspond to the resonant frequency of the magnet in order to generate electricity, see Figure 2. [49]

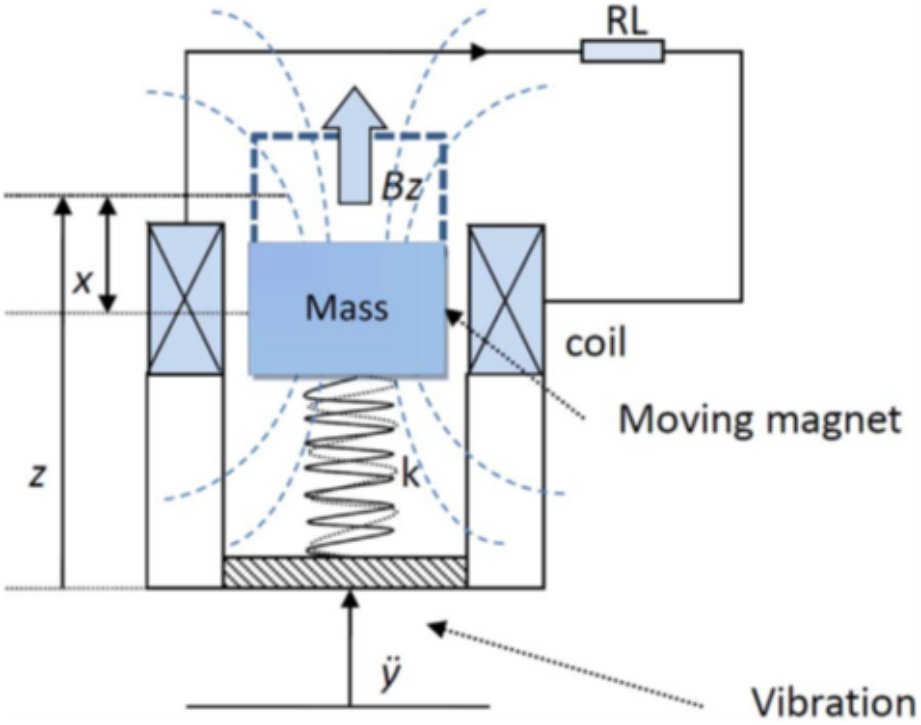

Figure 1: Workings of a electromagnetic energy harvester[49]

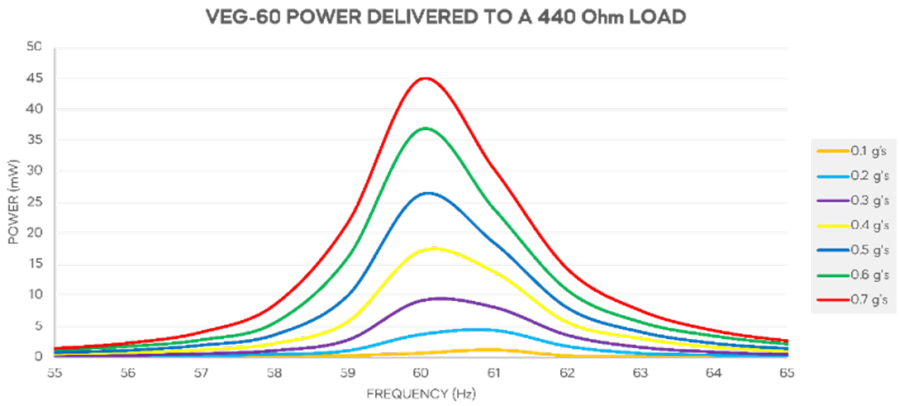

Figure 2: Plotted power output of a VEG-60 vibration energy harvester at different frequencies oscillating with different acceleration[49]

Note that electromagnetic energy harvesters can only harvest movement going in one dimension. This in conjunction with the output of the harvester

being heavily dependant on the frequency of the kinetic vibrations, makes electromagnetic harvesters only applicable in specific cases.

2.1.2 Photovoltaic energy harvester

Light harvesters operation is based on the photovoltaic effect. When a semiconductor PN junction is hit by light photons, part of their energy is absorbed by the semiconductor material releasing free electrons and creating an electric potential across the union. If the circuit is closed this voltage will generate a current flow through the circuit that goes from the N semiconductor terminal to the P terminal, see Figure 3. Light energy harvesters are more commonly known as solar cells or solar panels.[5]

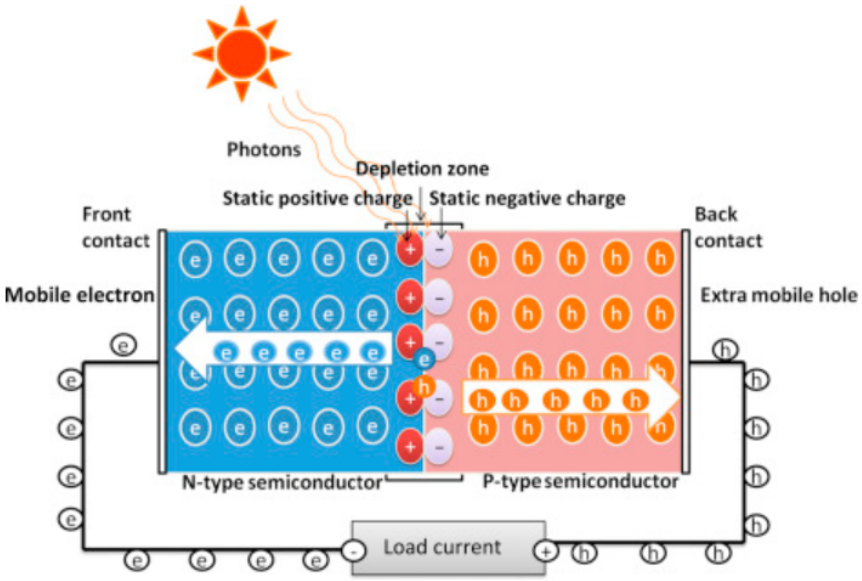

Figure 3: High level workings of a photovoltaic cell[5]

As of 2020 the energy conversion efficiency for solar cells ranges from 13.0% to 47.1% for different technologies, according to USA's National Renewable Energy Laboratory[5], see Figure 4. The conversion efficiency describes how much of the absorbed light energy is transformed to electric energy by the solar cells under best operating conditions.

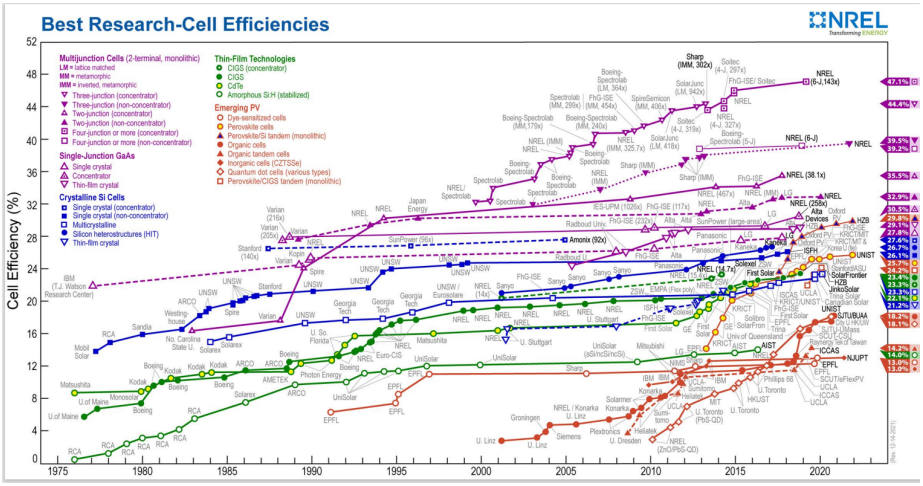

Figure 4: Evolution of energy conversion efficiency for different solar cell technologies[5]

Like other types of harvesters, the generated output power for solar cells depends on many different factors. However the most crucial is the exposure to a high-power light source, which may not be the case in indoor environments. Despite this, Nordic Semiconductor they were able to harvest 244µW in an indoor environment with 560Lx illuminance, using a generic 6x6cm solar cell, according to information provided by Nordic Semiconductor blog post[33]. The generated power from the cells is also dependent on the perpendicularity of the solar panel to the light source, as well as temperature and environmental conditions (e.g. clouds, rain or dust).

Solar cells can be found in all sort of sizes, formats, and output powers from a few tenths of micro Watts to hundreds of Watts. In the scope of low-power IoT devices panels with up to 0.5W of output power can be found for dimensions less than 10x10cm.[48] The main disadvantage of light energy harvesters for very long lifespans is the ability of the transparent layers that protect the cell's photo sensitive material to keep their transparency and light absorption properties over the product lifespan.

2.1.3 Heat energy harvesting

Heat energy harvesters generate energy in one of two ways, either from temperature differences of two surfaces (thermoelectricity) or from temperatures fluctuations over time (pyroelectricity).

Pyroelectric generators or PEGs generates energy from fluctuations of the temperature of the harvester over time in form of heating and cooling cycles. Today, this technology is being researched and there are no available commercial solu-

tions yet[13].

Thermoelectric generators, TEGs or also known as Peltier cells, generates energy using the Seebeck effect. The Seebeck effect is when two semiconductors with different temperatures produces an electrical potential between them.[13].

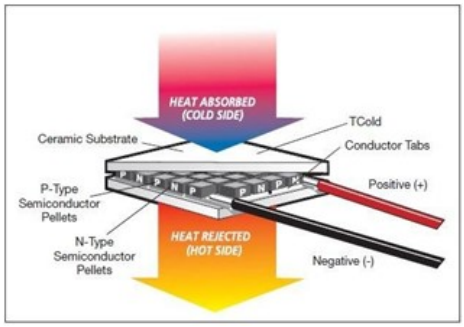

Figure 5: Schematic representation of a thermoelectric generator (TEG).

To maximize the Seebeck effect power output the TEGs are typically constructed of several thermocouple unions using materials that have low electrical resistance but high thermal resistance, an example of such material is the semiconductor Bismuth-telluride. These unions are sandwiched in between two ceramic plates, see Figure 5. By maintaining each plate at a different temperature, an electrical current can be extracted from the terminals. Maintaining the difference in temperature is crucial since both sides would reach the same temperature overtime due to heat transfer through the materials. The operation of TEGs can be reversed to act as an electric controlled cooling or heating element in which is known as the Peltier effect.[13]

TEGs generally has a comparatively low energy conversion efficiency which ranges between 1% to 15% depending on the source of information. Conversion efficiency is also directly proportional to the temperature difference between sides. Despite this, due to their flexibility and scalability potential, commercial TEGs can be found with power output ranging from the teens of microWatts to multipe milliWatts per degree of temperature difference depending on construction and dimensions.

Main advantages of TEGs are their solid-state construction (lack of moving parts), and great scalability. However, they lack on energy conversion efficiency and power output, especially for small temperature differentials, see Figure 6. On top of that they can be quite fragile and must be installed properly to ensure very good heat transfer.

Type	ACR	RT	TEG Output per 1deg dT			TEG Top Ceramics		TEG Bottom Ceramics		Height
	Ohm	K/W	E1 mV	I1max mA	P1max uW	A mm	B mm	C mm	B mm	H mm
1MC06-126-xx_TEG										
1MC06-126-15_TEG	10.8	11.1	50.4	2.33	58.72	16.0	16.0	16.0	16.0	2.6
1MC06-126-12_TEG	8.7	8.9	50.4	2.91	73.40	16.0	16.0	16.0	16.0	2.3
1MC06-126-10_TEG	7.2	7.5	50.4	3.50	88.08	16.0	16.0	16.0	16.0	2.1
1MC06-126-08_TEG	5.8	6.0	50.4	4.37	110.10	16.0	16.0	16.0	16.0	1.9
1MC06-126-05_TEG	3.6	3.8	50.4	6.99	176.16	16.0	16.0	16.0	16.0	1.6

Figure 6: Device characteristics and performance metrics for of the shelf thermoelectric generators[30]

2.1.4 Radio frequency energy harvesting

Radio frequency energy harvesting captures radiated electromagnetic energy, such as those generated by digital TV, LTE, Wifi transmissions, through an antenna. Since this project anticipates to create an energy neutral IoT device it will focus be on harvesting energy from ambient sources and not harvesting energy from a dedicated transmitter. Note that energy can only be harvested when data is transmitted which is not always the case depending on the type of signal.[28]

The signal strength is highly dependent on the terrain and the distance between the transmitter and receiver.

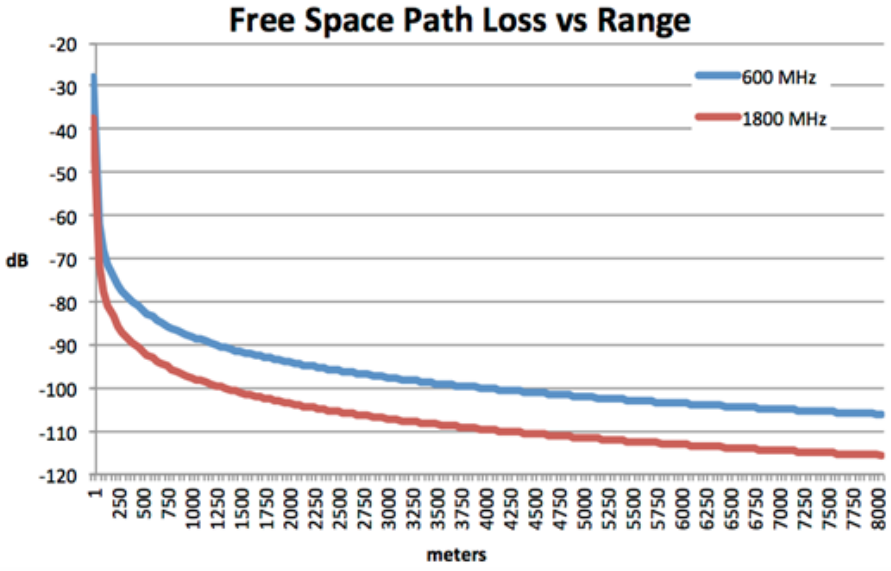

Figure 7: Free space path loss vs range[28]

Lower frequency signals are less attenuated over greater distances, but we can see in Figure 7 both signal strengths fall off quite fast in the first 250 meters.

Freq. (MHz)	Application	Wireless Power Capture by Dipole (microwatts)
560-580	Digital TV	18.54 - 30.76
540-560	Digital TV	39.02 - 64.76
520-540	Digital TV	21.44 - 35.58
510-520	Digital TV	0.007 - 0.011
494	Analog TV	8.88 - 14.74
487	Analog TV	49.77 - 82.60
480	Digital TV	51.23 - 85.03

Figure 8: Measured power levels that could be exploited by an radio frequency harvesting circuit[28]

Figure 8 describes the measure power levels of different transmissions and frequencies, where the radio transmitter is 6.5 km away and has a transmitting power of 100 kW. Note that this is direct line of sight and free space. In an urban environment there is many different types of transmissions and therefore more possibilities for harvesting radio frequencies but there is also a lot more obstacles which will lower the signals strength.

A master thesis project tested radio frequency energy harvesting at frequencies of 0.8, 0.9, 1.8 and 2.4 GHz (at the same time) at four different locations in Sweden[43], see Figure 9.

Location Number	Description
Location 1	Inside, in a window facing a Tele2-transmitter with an approximately distance of 100m.
Location 2	Outside facing a tower with multiple cellular transmitters with an approximate distance of 200m.
Location 3	Outside facing a tower with multiple cellular transmitters with an approximate distance of 400m.
Location 4	A typical location outside in a city environment with an unknown distance of the closest transmitter.

Figure 9: Descriptions of locations tested in the master thesis project[43]

Location Number	Maximum harvested energy	Average harvested energy
Location 1 (Indoor)	35μW	10μW
Location 2 (400m)	0.5 μW	0.35 μW
Location 3 (200m)	1 μW	0.7 μW
Location 4 (City)	0 μW	0 μW

Figure 10: Recieved power from the different locations presented in the master thesis project[43]

Results shown in figure 10 describes both maximum and average energy harvested. In these measurements we can see that the distance greatly affects the signal strength and therefore the harvested energy. As we can see be the measurements taken in a city environment (Location 4), the effects of terrain and structures decreases the energy harvested.

Comparing the energy harvested from ambient non-dedicated radio frequency signals in the two papers, we can conclude that the harvested energy is highly dependent on the receiver's location and surroundings as well as the transmitters transmitting power. Maybe this could be used as a stable source of energy, but the scenario seems very niche.

2.1.5 Electromagnetic induction

Electromagnetic induction harvests energy according to Faraday's law. When a coil is placed within a changing magnetic field a current will be induced to the coil. See Figure 11 for an example setup for an electromagnetic induction harvester.

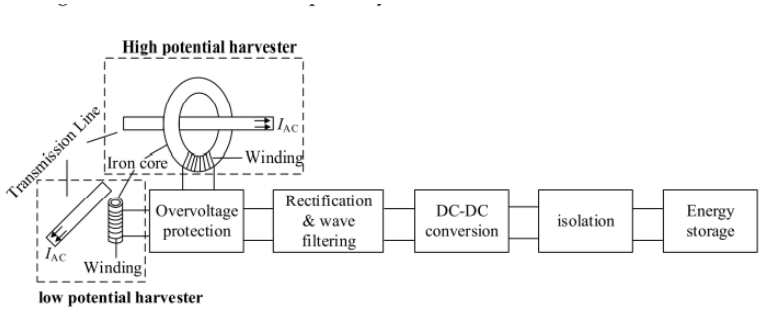

Figure 11: Example of setup on an eletromagnetic induction harvesting device. [46]

The master thesis "Power Line Induction Energy Harvesting Powering Small Sensor Nodes"[46] used six different types of inductors to harvest a power line

with a current of 13A, voltage of 230V oscillating at 50Hz (typical household electric installation), see Figure 12. Different inductor dimensions and core material were used and placed "close" to the power line. The harvested power for each inductor and core combination in mW can be seen in Figure 12.

Inductor	Air	Ferrite	Ferrite × 2	Ferrite × 3
1	200	313	432	432
2	57	213	313	529
3	56	262	385	0.66
4	0.08	0.39		
5	0.04	0.36		
6	0.03	0.37		

Figure 12: Description the measured power levels, in mW, from six types of inductors using different cores, harvested on a 230V 13A 50Hz transmission line

An induction harvester can be a highly stable, cost effective and high-power harvesting system. However, the use case of it only applies to niche applications since it needs to be located near a current carrying structure, making it a main disadvantage of induction power.

2.1.6 Summary of harvesters

There is no universal solution for energy harvesting that can meet the energy requirements and operating environments of all kinds of applications. Some technologies are better suited than others for particular cases.

Light harvesting seems to be a strong option for many use cases as it generates a considerable amount of energy as long as it receives enough light. Vibration harvesters also show considerable power generation capability but depend on resonance operation, thus their output would be greatly reduced for scenarios with random vibration patterns.

Heat harvesting using TEGs is also able to deliver "high" energy levels, but care must be taken to ensure a continuous temperature gradient over time. Radiated radio frequency harvesting would only be feasible for ultra-low power applications and new technologies have be developed to enable wireless communications powered by it. Lastly, electromagnetic inductive harvesting could perhaps harvest the highest amount of energy compared to the other options but is completely dependent in the presence of strong oscillating electromagnetic fields and correct placement of the device.

Considering the purpose of this master thesis, the most suitable option would be kinetic and light energy harvesting due to their output power levels and availability on the application's environment. Kinetic energy would be present in the vibration of the shopping cart structure while moving, whereas light energy would be provided by sunlight when the cart is outdoors and artificial light when indoors.

2.2 Energy storage

Since none of the harvesters are reliably able to provide an IoT device with enough constant power, an energy source is needed to store the harvested energy. Batteries and super capacitors are two ways of storing electric energy. When comparing batteries and super capacitors, the following factors have been recognized as the main considerations:

- Energy gravimetric density
- Capacity retention
- Lifespan
- Materials

2.2.1 Energy gravimetric density

Energy gravimetric density is a unit that describes how much energy per weight an energy storage has. Energy gravimetric density is often measured in $\frac{Wh}{Kg}$.

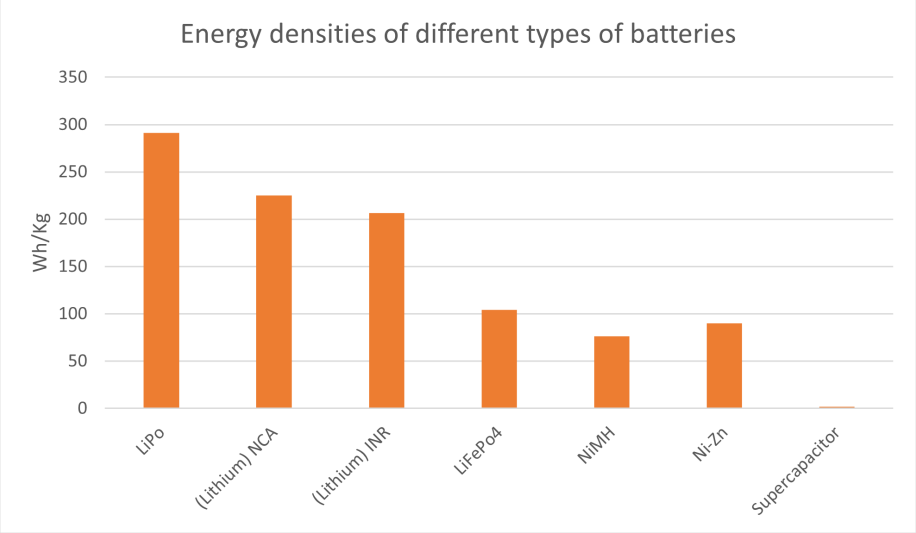

Figure 13: Diagram of energy gravimetric density of different kinds of batteries and super capacitors

In several comparisons of the energy gravimetric density of batteries with different chemical compositions and super capacitors, the lithium based batteries was concluded to have the greatest energy gravimetric density. The super capacitors energy gravimetric density was not even comparable to the nickel based batteries with a density of around 3 $\frac{Wh}{Kg}$, see Figure 13. Data gotten from [35] [42] [19] [20] [21] [22] [23] [3] [39] [4] [7] [38] [11] [18] [2] [1] [37]

2.2.2 Capacity retention

The main issues with batteries compared to super capacitors are that batteries capacity retention decreases during cycles of charges and discharges.

In figure 14 the capacity retention of a litium ion battery is depicted over the number of charging cycles. There are multiple graphs describing the capacity retention after being charged and discharged between different states of charges at temperatures around 30 degrees Celsius. One can see that the degradation is not as strong when only cycling closer to a state of fully discharged compared to close the state of fully charged.[51]

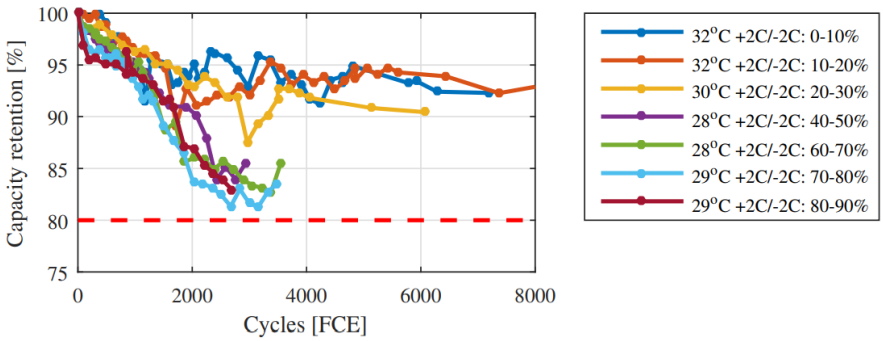

Figure 14: Capacity retention versus the number of cycles[51]

According to vendor data sheets the super capacitors capacity retention is vastly greater than the batteries capcity retention.

2.2.3 Materials

A lithium ion battery, depending on the chemistry used, often contains lithium, cobalt, nickel and copper. These metals are not generally considered toxic, especially compared to lead and cadmium batteries. The extraction of lithium on the other hand is a hazardous process. Lithium extraction consumes 500 000 gallons of water per ton of lithium [36]. On multiple occasions dead fish have been reported as a result of toxic chemical leak of different lithium mines. Furthermore, recycling of lithium batteries is not common (e.g. only about

2% of Australia's lithium waste is recycled). This is because degraded lithium cathodes cannot be reused in batteries and there is no efficient way of turning batteries into the raw metals again.[36]

One of the biggest advantages for supercapacitors is the life span, which so much better than batteries. This contributes to less waste and less extraction of possibly toxic materials [9]. Supercapacitor's chemistry, just like batteries, differs greatly between different types of supercapacitors and therefore has different environmental impacts. Metallic supercapacitors are generally regarded as containing materials that are very toxic towards the environment, but supercapacitors based on carbons and polymers are considered "environmentally safe". Note that we have not found data on the recycling of supercapacitors. [41]

Hence, in an environmental perspective, the carbon and polymer-based supercapacitors are the best choice for this project.

2.3 Low power communications

There are a lot of network communication options for low power embedded systems such as are LTE-M, NB-IoT, Bluetooth low energy, Bluetooth mesh, Wi-Fi, Wi-Fi HaLow, LoRaWAN, Sigfox, Zigbee and MIoTy. The main networks investigated has been LTE-M, NB-IoT, Bluetooth low energy, Sigfox and LoRaWAN. The important characteristics of a low power network are availability and power consumption. The availability of a network is primarily decided by the coverage of a base station and the implemented infrastructure available of that network. The power consumption of a network is mainly dependant on the energy management and the data throughput. Therefore the areas of comparison have been focused on coverage, data throughput and energy management.[24]

2.3.1 Infrastructure and coverage

The coverage of a network is dependant on many factors such as transmission power of both the base station and the connected node, what network band they are communicating over, sensitivity of the antennas, the present environment and the number of base stations.

LTE-M and NB-IoT LTE-M and NB-IoT has a big advantage to other networks in regards of coverage, since it is based upon a 3GPP standard and uses the already available LTE base stations. This can be seen by a coverage map provided by Telia, both their LTE-M and NB-IoT network has a good coverage over Stockholm, see Figure 15 and 16.

Figure 15: Telia LTE-M network coverage[45]

Figure 16: Telia NB-IoT network coverage[45]

LoRaWAN

LoRaWAN network is available in 160 countries[32] worldwide. However, it is mostly available as smaller local installations. As of this, it would not be a reliable network unless a LoRaWAN base station would be deployed nearby. A LoRaWAN base station can provide up to 15 km of range according to "Semtech"[50].

Sigfox

Sigfox network is available in 70 countries[32] worldwide. However, the number of base stations per country is not high enough to be regarded as reliable, especially in rural areas. A Sigfox base station can provide up to 40 km of range[29].

Bluetooth low energy and WiFi

Bluetooth low energy and Wi-Fi are made for local and personal networks, hence, it does not support nearly as big of a coverage. Wi-Fi supports up to

about 200 meters and Bluetooth low energy is in the range of 10s of meters. Bluetooth mesh can solve the range issue of Bluetooth but requires all nodes to always be active or make use of "friendships" where an always on node (relay node) stores requests to low power nodes that might be in sleep mode.

2.3.2 Data throughput

The data throughput, or data rate of a network, has a big impact on the overall power consumption of a modem since the data rate is directly affecting the time the modem is active. See Figure 17 to see data rate of different network technologies.

Technology	Sensitivity	Data rate	Spectrum Strategy
WiFi (802.11 b,g)	-95 dBm	1-54 Mb/s	Wide Band
Bluetooth	-97 dBm	1-2 Mb/s	Wide Band
BLE	-95 dBm	1 Mb/s	Wide Band
ZigBee	-100 dBm	250 kb/s	100 m
SigFox	-126 dBm	100 b/s	Ultra Narrow Band
LoRa	-149 dBm	18 b/s - 37.5 kb/s	Wide Band
Cellular data (2G,3G)	-104 dBm	Up to 1.4 Mb/s	Narrow Band

Figure 17: Sensitivity, data rate, spectrum strategy of different networks according to [34]

2.3.3 Energy management

Managing the power consumption of a network modem is crucial when trying to use as little energy as possible. All networks investigated has some sort of low power modes or allows the user equipment to sleep to lower the power consumption when the modem is not either transmitting or receiving data.

LTE-M and NB-IoT

Both of the 3GPP standard networks LTE-M and NB-IoT has two different low power modes, power saving mode (PSM) and extended discontinuous reception (eDRX). 3GPP also specifies an energy saving feature called release assistance indication for both networks.

In PSM this is achieved through putting the modem into dormant mode where

it cannot receive any traffic, however it can at any time wake up and transmit data. After each transmission the modem might go into a active window where the modem is reachable for a while until it goes back to dormant mode. If it is dormant for too long the modem must wake up to send a tracking area update (TAU)[8], see Figure 18 The duration of the active window and the TAU interval is requested by the modem on first connect but regulated by the network operator.

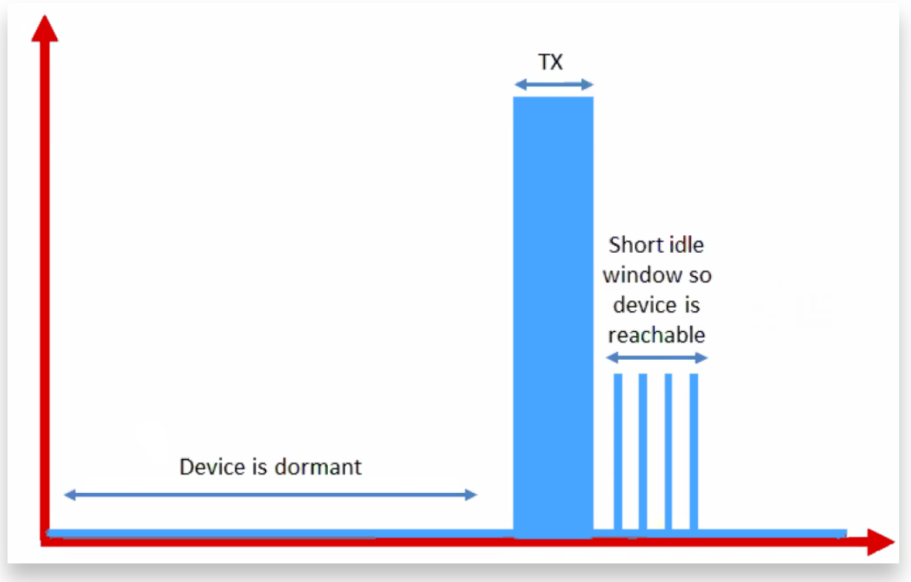

Figure 18: Illustration of power saving mode (PSM)[8]

The eDRX also achieves lower power consumption by the modem while still being able to receive incoming data. This is done through a permanent paging interval where it can receive messages which is queued by the core network, see Figure 19. A larger duration between different pages causes lower power consumption, but the latency of the data increases. How often the modem should page is also requested by the modem on first connect but regulated by the operator[8].

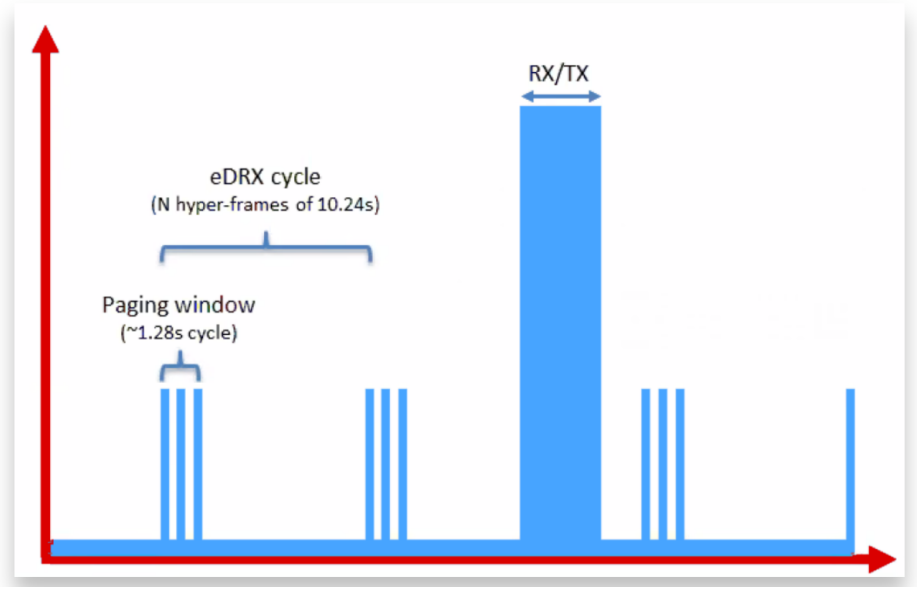

Figure 19: Illustration of extended discontinuous reception (eDRX)[8]

A possible problem for the 3GPP networks energy management and consumption is the network timers that describes the connection characteristics of the modem. The main ones are:

- RRC - For how long the radio resource control should be active after a modem activity.
- idle mode Discontinuous Reception (iDRX) duration - For how long the iDRX should last after a transmission.
- idle mode Discontinuous Reception (iDRX) page interval - How often the modem should page during the iDRX.
- extended Discontinuous Reception eDRX duration - For how long the modem should stay in sleep mode between pages.
- TAU - For how long can the modem be in PSM mode before it needs to wake up to do a tracking area update.

Most of these timers can be requested to the network (except RRC timer), but there is no guarantee that the requested timers will be received because they are regulated by the operators themselves. These timers have a great affect on the power consumption of the modem.

Release assistance indication or RAI released in 3GPP release 14.RAI is a way for the UE to reduce the radio resource control connection time by telling the

network that it does not expect any more downlink or uplink communication. There are two main configurations of RAI:

- No more uplink or downlink - Often used in connectionless network protocols such as UDP
- A single downlink transmission and no more transmission - Used when the network expect a response or acknowledgement, i.e. TCP

LoRaWAN, Sigfox, Bluetooth low energy & WiFi

All the networks above support the network modem to go into sleep mode and turn off the radio when not transmitting or receiving any data. This means that the user equipment itself has full control over the modem status and therefore the power consumption.[24]

2.4 Network communication protocol

No matter what type of network the user equipment uses one can choose multiple communication protocols in both the IP layer and the application layer. The main considerations of choosing a network protocol to use for the user equipment is purpose, overhead and reliability. The main protocols investigated in this thesis are:

- User datagram protocol (UDP) [Transport]
- Transmission control protocol (TCP) [Transport]
- Constraint application protocol (CoAP) [Application]
- Message queuing telemetry transport (MQTT) [Application]

2.4.1 User datagram protocol (UDP)

User datagram protocol or UDP is a simple transport layer protocol with low overhead, see Figure 20. UDP does not provide any reliability but does provide a checksum in the UDP header that is used to make sure the data is not corrupted over transmission. [15]. UDP does not require any communication prior to sending data and can send data directly with one packet.

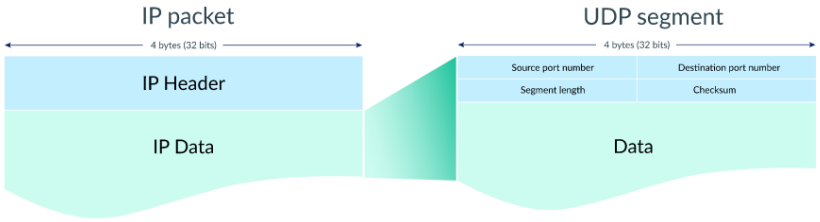

Figure 20: UDP packet

2.4.2 Transmission control protocol (TCP)

As UDP, TCP is an Transport layer protocol.In contrary to UDP, TCP is made to ensure reliability of packets using the larger TCP header[40], see Figure 21.

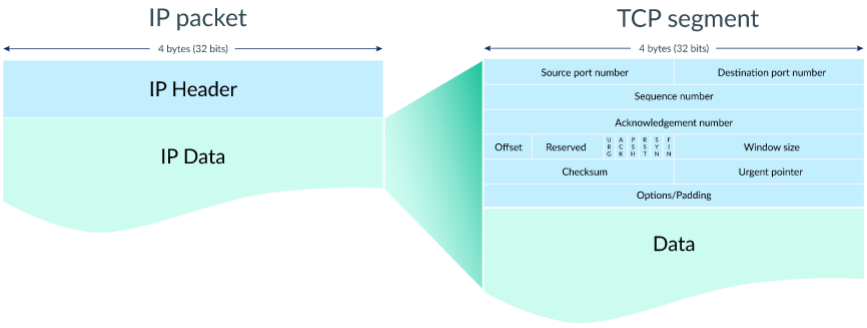

Figure 21: TCP packet[14]

Prior to sending data the two involved machines must synchronize by doing a so called handshake, see Figure 22. The handshake is consistent of three messages without data: a SYN message from machine 1, a SYN ACK from machine 2 followed by a ACK from machine 1 when sending data from machine 1 to machine 2. The type of messages is determined by the active bit(s) in the "flags" part of the header. This handshake is made before all transmissions to ensure a working connection.

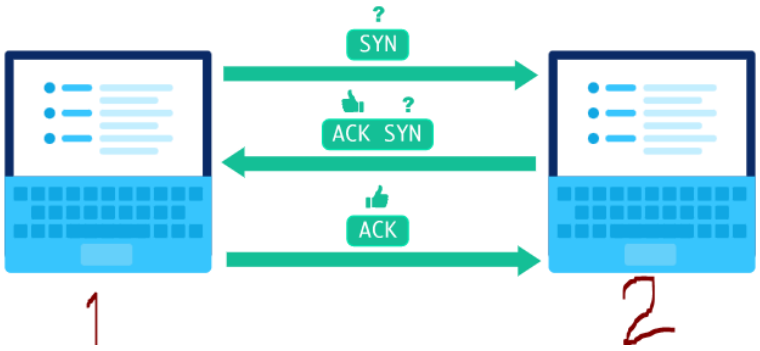

Figure 22: Initial TCP handshake[14]

All data that is sent contains a sequence number which must be acknowledged by the receiving machine to keep track of which packets that has been received successfully or not, see Figure 23.

Figure 23: Sending data over TCP

Using these acknowledgements and sequence numbers together with timers a machine can understand if packets get lost and do a retransmission.

Compared to UDP, TCP adds a lot of overhead, both in the actual TCP header and in the number of transmissions to get the data to the other end.

2.4.3 Constraint application protocol (CoAP)

CoAP is an application layer protocol made for resource constraint devices. It is a one-to-one communication protocol based upon the request-response model[16] It is similar to HTTP but ensures less overhead, see Figure 24. Unlike HTTP the underlying transport layer protocol used is UDP[47].

Message		Header size (B)	
		CoAP	*HTTP*
cacerts	request	6–26	> 160
	response	3	> 118
enroll	request	8–28	> 235
	response	3	> 125

Figure 24: CoAp vs HTTP header size[17]

2.4.4 Message queuing telemetry transport (MQTT)

MQTT is an application layer protocol that makes use of the publish/subscribe architecture [31]. The concept is that the system consists of a group of clients and brokers. The clients can both subscribe and publish to a brokers topic. When a broker receives a publication to a topic it sends data out to all of the topics subscribers. See Figure 25

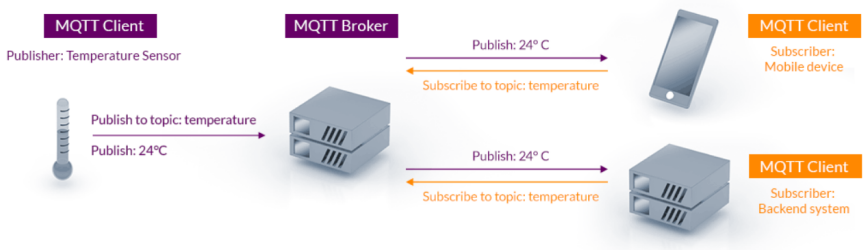

Figure 25: Publish subscribe architechture[31]

The message will be stored until all receivers have received the message. The underlying transport layer protocol used is TCP. This means that MQTT ensures that the data will be received by a subscriber even if the packet is lost in the air or the device itself is currently not listening.

2.5 Global navigation satellite system (GNSS)

Global navigation satellite system or GNSS is a system that provides a user with precise position. This is done with triangulating the distance to a minimum of three satellites with known positions. The distance is calculated by the speed of a transmission (speed of light i.e. radio frequency transmission) and the time of arrival of a transmission:

$$distance = c * (t_{received} - t_{sent})$$

The time of received transmission, $t_{received}$, is not accurately known. This is calculated through a fourth satellite[44]. This data is then returned to the user as PVT (position, velocity and time) data.

There are multiple GNSS systems available with this implementation across the globe. GPS, GLONASS, Beidou and Galileo are the most common ones. The main problem with GNSS is the first time a device is acquiring a fix. This is referred as Time-to-first-fix (TTFF) or a 'cold start' and can take a lot of time which corresponds to a large power consumption[6].

There are services to fix this 'cold start' issue called assistance GNSS. This works by receiving time and ephemeris satellite data over the internetwork instead of the satellite communication link. The networks bandwidth is vastly greater than the satellite connection which results in a much better TTFF or 'cold start'.

2.5.1 Carrier-to-noise density (CN0)

Signal-to-noise ratio, or SNR, is as the name states the ratio between the signal strength and surrounding noise in a certain bandwidth measured in dB. Carrier-to-noise density is measured in dB/Hz and is the ratio between carrier power and noise power density which is the noise power per hertz[26].

3 Methodology

The main purpose of this project was to design and create a prototype that could acquire GNSS position and transmit over LTE-M or NB-IoT, by using harvested energy that otherwise would go to waste. As presented in chapter 2, a research overview of related areas was done to collect relevant knowledge. The research overview resulted in four main considerations for this project:

- What harvester(s) to use
- What network to use
- What network protocol to use
- What network timers to request

3.1 Current measurement

To measure the current consumption of the nrf9160 SiP the nordic semiconductor power profiler kit 2 (ppk2) were connected to the nrf9160dk. Using the nordic semiconductor power profiler v3.4.2 software the current consumption could be recorded. The measurements only measures the consumption of the nrf9160 SiP and not the whole board.

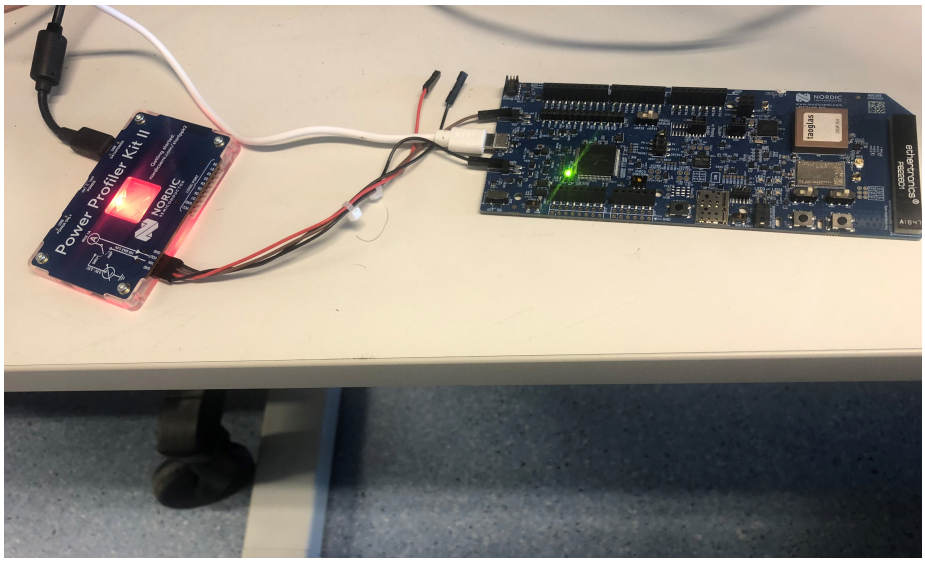

Figure 26: Ppk2 connected to the nrf9160dk

Measurements was made by programming small test programs that only does one particular thing. The test programs made was:

- Network connect and attach

- Network transmission using TCP
- Network transmission using UDP
- GPS acquisition

3.2 Harvesters

Based on the research of related work, the types of harvesters best suitable for the prototype is an electro magnetic vibration energy harveter, a photovoltaic panel or a combination of both depending on the harvesters power output. The harvesters power output was measured under different circumstances. To analyze the output, a python script was created to do calculations to convert the voltage to power and energy. The oscilloscopes used was tested to make sure that they were calibrated correctly.

To measure the vibration energy harvester power output, two setups was created. Firstly an indoor setup using a sin wave generator connected to a vibrator. The output of the VEH was then connected to an oscilloscope.

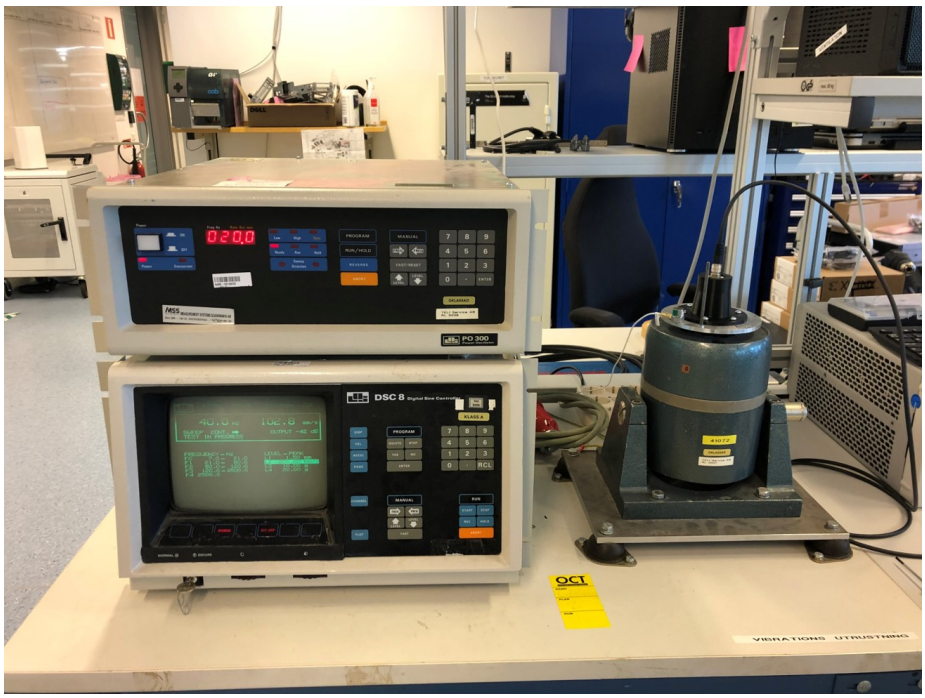

Figure 27: VEH mounted on a vibrator powered by sine wave generator

The indoor setup was to test the power output at different loads, frequencies and accelerations.

An outdoor setup was also created where the vibration energy harvester and a thingy91 was mounted on the shopping cart. The thingy91 was programmed to work as an accelerometer that logged vibrations from the shopping cart and was connected to a computer in the shopping cart. A mobile usb-connected oscilloscope (called PicoScope 2206B) was also connected to the computer, measuring the VEH output.

Figure 28: Outdoor setup

Figure 29: Thingy91 and vibration energy harvester mounted on the shopping cart

The outdoor setup was used to measure the shopping cart vibration characteristics and the power output of the VEH. The data was gathered from the vibrations generated by the shopping cart being walked over asphalt at different speeds. In all measurements of the VEH there was a load of 100 Ohms connected to the output of the harvester.

3.3 Networks

Since this project is a co-operation with Ericsson our network choices were limited to either LTE-M or NB-IoT.

Figure 30: Ericsson LTE Radio

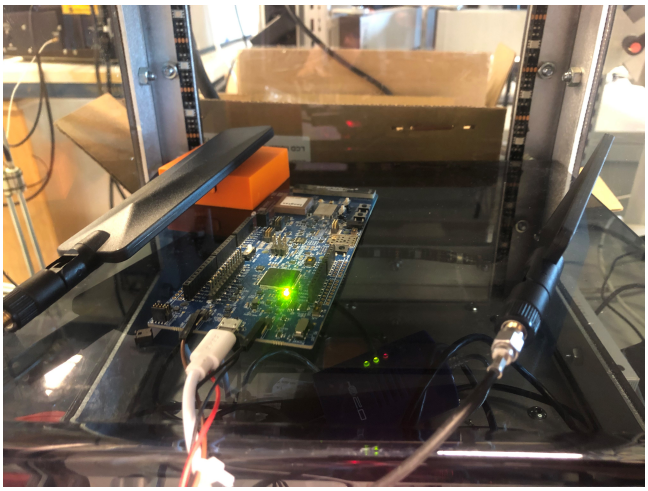

Figure 31: Antennas put into the an isolated box

To be able to choose between these two networks, a network was setup in a box isolated to radio frequency interference where full control was obtained over the network. The power consumption of low power modes and transmissions was then measured with the two networks using different network timers and network protocols. The radio and and the inside of our isolated box is shown in pictures 31 and 30.

3.4 Mounting bracket

Since the shopping cart is vibrating quite a lot when moving, all components, except the vibration energy harvester, was mounted on a suspended bracket to avoid damaging the components. All components were visible for demonstrating purposes. A LTE connected tablet was used to visualize the positional data and the voltage of the energy storage.

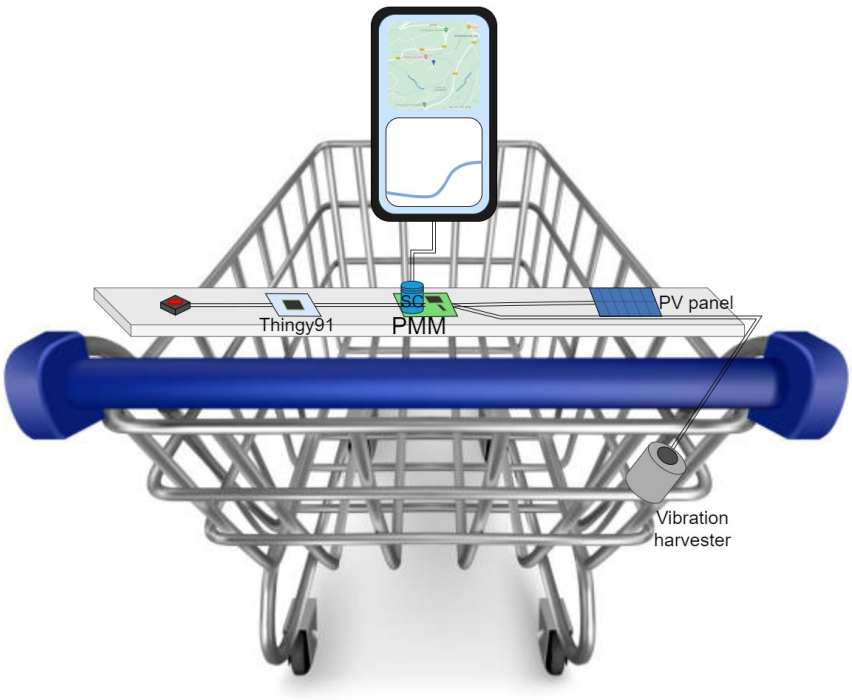

Figure 32: Idea of the mounting bracket

4 Current measurements

To get an understanding of the power consumption, a series of current measurements were made for different parts of the network segments and GNSS acquisition. All current measurements are measured on the nrf9160dk usin the *Nordic Semiconductor power profiler kit 2 (ppk2)*. The power profiler kit 2 only measures the current consumption of the nrf9160 SiP and not the whole board with all it's peripherals. The ppk2 is sampling the current at a sampling rate of 10 000 samples per seconds. The supplied voltage during the measurements is constant at 5V. The GPS acquisition time is very inconsistent, the time can be all from 1 second to over 40 seconds depending if it is a hot start, cold start, the angle of the antenna and the environmental conditions. Even though the GPS acquisition time is very inconsistent the current consumption is consistent during this interval. The times of different network segments, for instance the continuous mode Discontinuous Reception (cDRX), is regulated by the operator of the network itself and can only be requested by the application. As of this, the times are of less importance compared to the current consumption itself.

4.1 Cat NB1 - transmission (UDP)

In the figure below the current consumption of transmitting a payload with the size of 64 bytes as a UDP packet over a NB-IoT network is shown. The measurements starts with the initial connection and tracking area update (TAU) followed by a big spike in consumption which is the transmission, finally a long constant consumption which is the continuous mode Discontinuous Reception (cDRX). The iDRX duration timer is set to 0 and therefore not present in this measurement. In the right corner the charge consumed by the grey highlighted area is measured at 194.93 milliColoumb (mC).

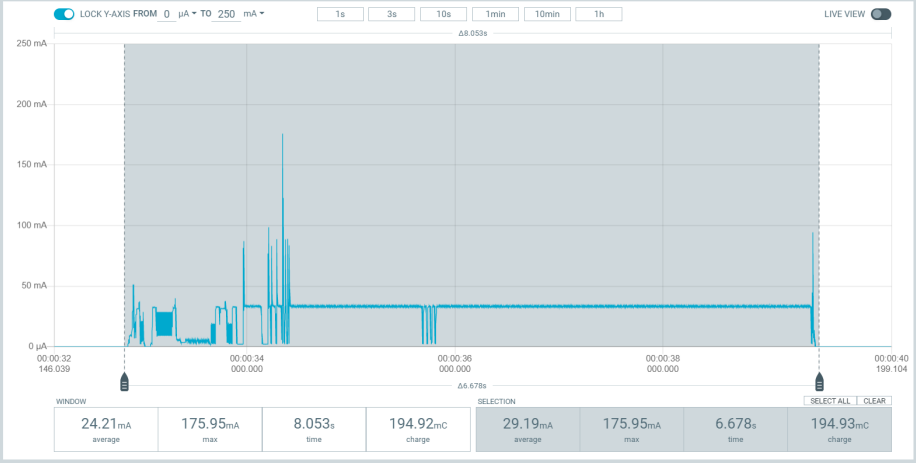

Figure 33: UDP packet transmission consumption over NB-IoT

4.2 Cat NB1 - transmission (UDP) using release assistance indication

Transmitting a payload with the size of 64 bytes as a UDP packet using release assistance indication (RAI) over a NB-IoT network. When using release assistance indication the cDRX duration is almost completely gone. The iDRX duration is set to 0. The charged consumed was 21.79 mC.

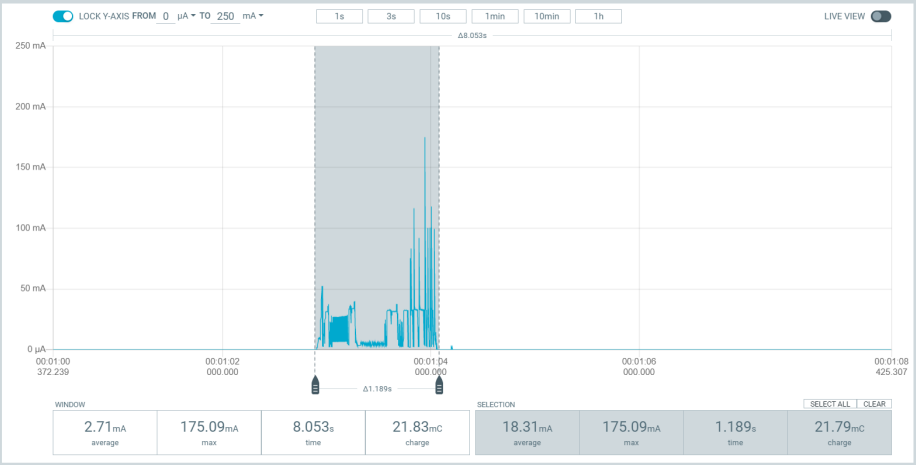

Figure 34: UDP packet transmission consumption over NB-IoT using release assistance indication

4.3 Cat NB1 - transmission (TCP)

The figure below shows the current measurement when transmitting a payload with the size of 64 bytes as a TCP packet over a NB-IoT network. The iDRX duration was set to 0 during this measurement. The charge consumed was 201 mC.

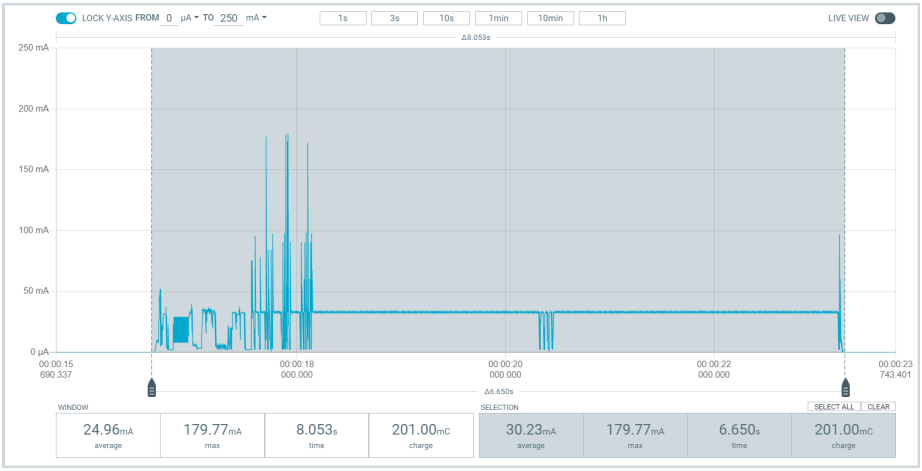

Figure 35: TCP packet transmission consumption over NB-IoT

4.4 Cat NB1 - transmission (TCP) using release assistance indication

Transmitting a payload with the size of 64 bytes as a TCP packet using release assistance indication (RAI) over a NB-IoT network. The charge consumed was 49.65 mC.

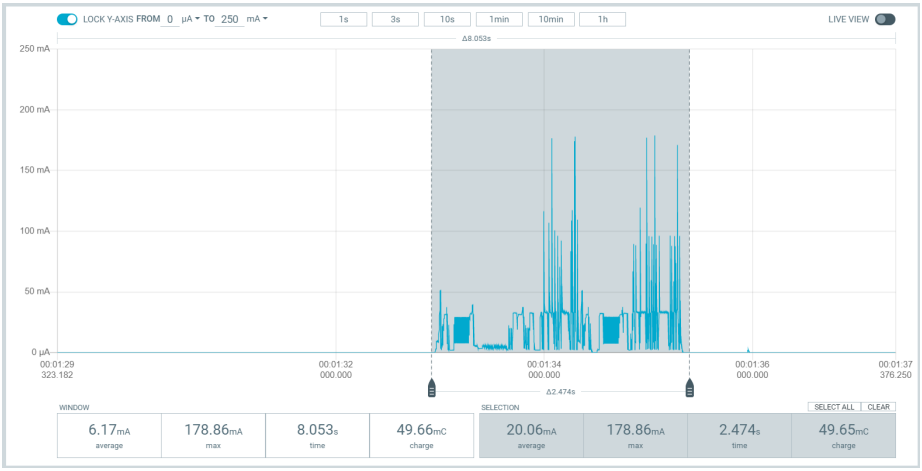

Figure 36: TCP packet transmission consumption over NB-IoT using release assistance indication

4.5 Cat NB1 - idle mode Discontinuous Reception (iDRX)

The current consumption when the modem is in idle mode DRX when connected to NB-IoT. The iDRX duration was not set to 0 and is using the default settings for this Telia NB-IoT network. The charge consumed was 6.64 mC.

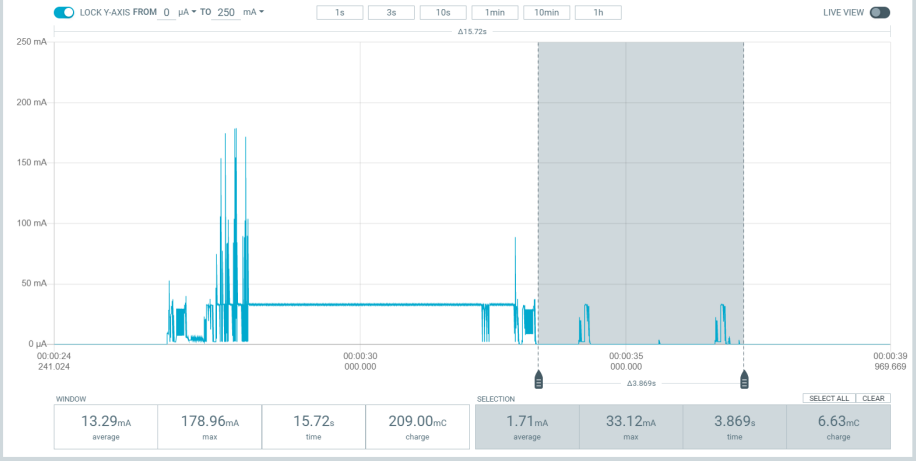

Figure 37: NB-IoT paging window consumption

4.6 Cat NB1 - PSM

The current consumption when the modem is in power saving mode whilst connected to NB-IoT. The average current consumption was around 2.33 microAmperes (μA).

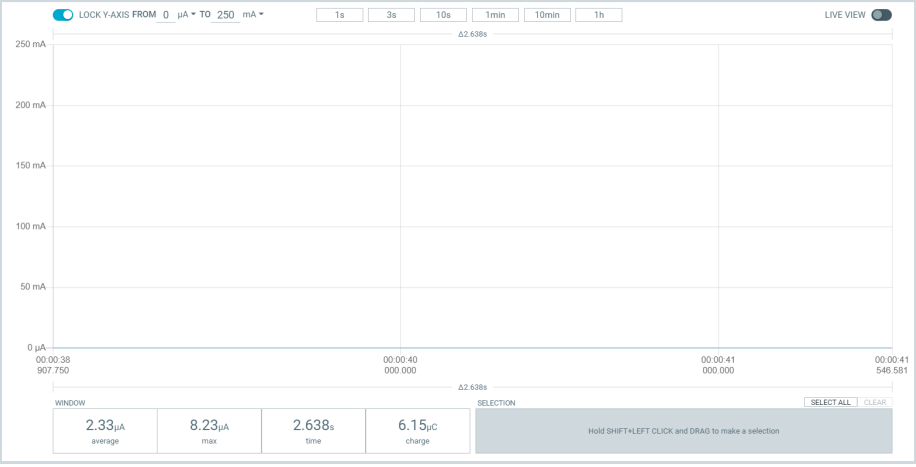

Figure 38: NB-IoT PSM mode consumption

4.7 Cat M1 - transmission (UDP)

Transmitting a payload with the size of 64 bytes as a UDP packet over a LTE-M network.

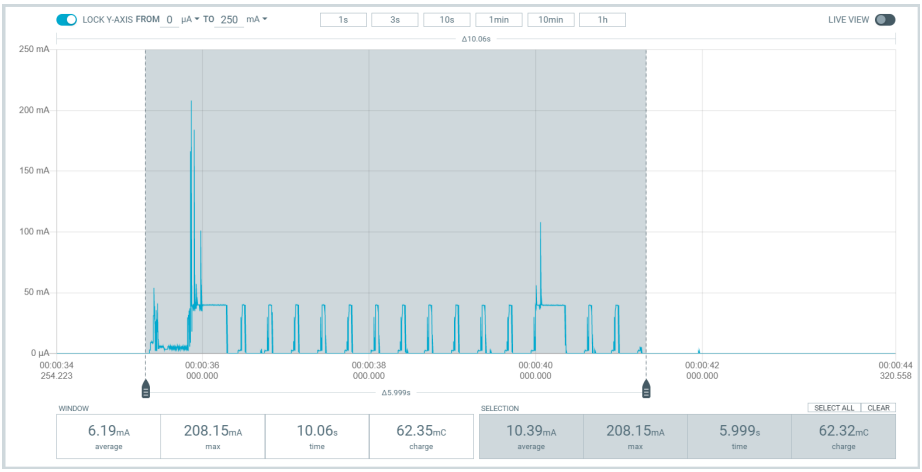

Figure 39: UDP packet transmission consumption over LTE-M

4.8 Cat M1 - transmission (TCP)

Transmitting a payload with the size of 64 bytes as a TCP packet over a LTE-M network. All current consumption measurements were taken at a constant 4V voltage supply.

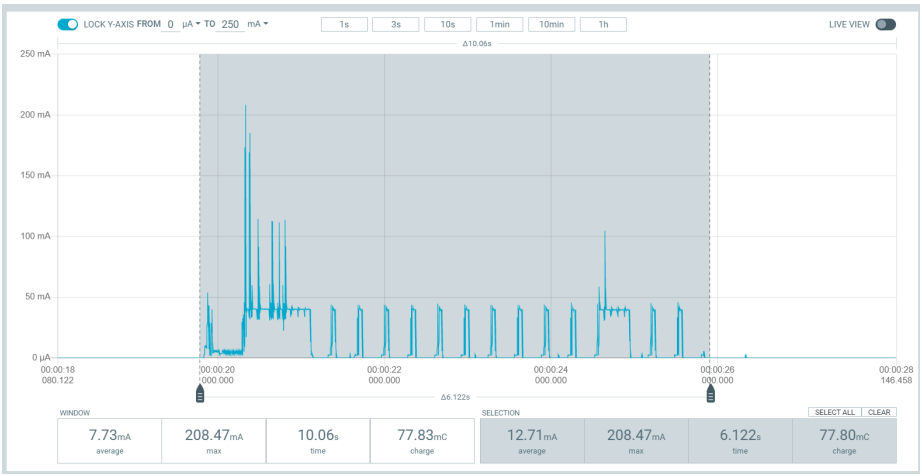

Figure 40: TCP packet transmission consumption over LTE-M

4.9 Cat M1 - idle mode Discontinuous Reception (iDRX)

The current consumption when the modem is in idle mode DRX when connected to NB-IoT. The iDRX duration was not set to 0 and is using the default settings for this Telia NB-IoT network. The charge consumed was 10.11 mC.

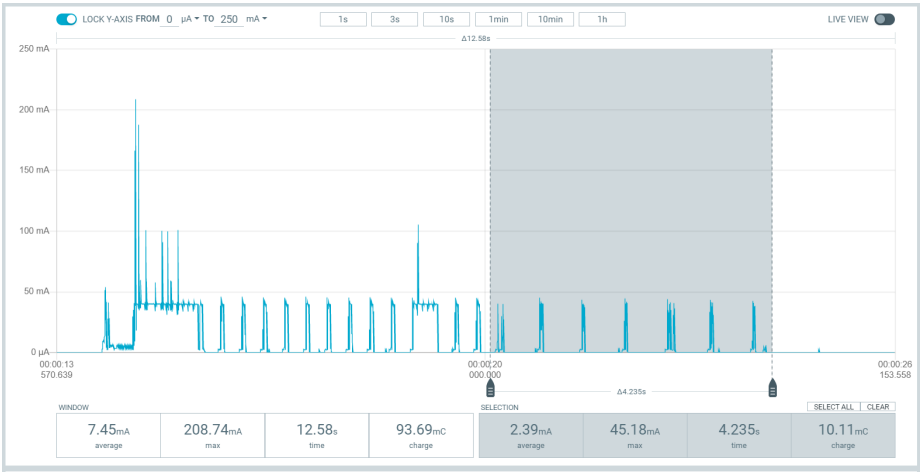

Figure 41: LTE-M paging window consumption

4.10 Cat M1 - PSM

The current consumption when the modem is in power saving mode whilst connected to LTE-M. The average current consumption was around 2.36 μA

Figure 42: LTE-M PSM mode consumption

4.11 GNSS

The figure below shows the current consumption whilst trying to acquire a geographical position. The current consumption is at average around 40.93 mA.

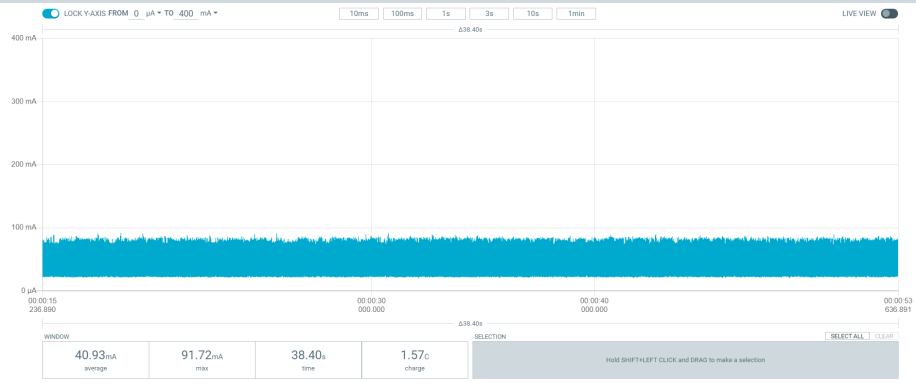

Figure 43: GNSS acquisition consumption

5 PMM design

To test the demonstrator, both a vibration energy harvester and a photovoltaic harvester (solar panel) are used. Both harvesters will have a separate power management circuit to maximize the power going into the energy storage.

The power output of the vibration energy harvester is a very small and inconsistent alternating current. These characteristics makes the output very hard to impedance match. Therefor all done to the alternating current is to rectify the current straight into the capacitor.

The power output of a solar panel is a relatively consistent direct current. The power output is dependant on the impedance of the system which can be shown through a current-voltage diagram.

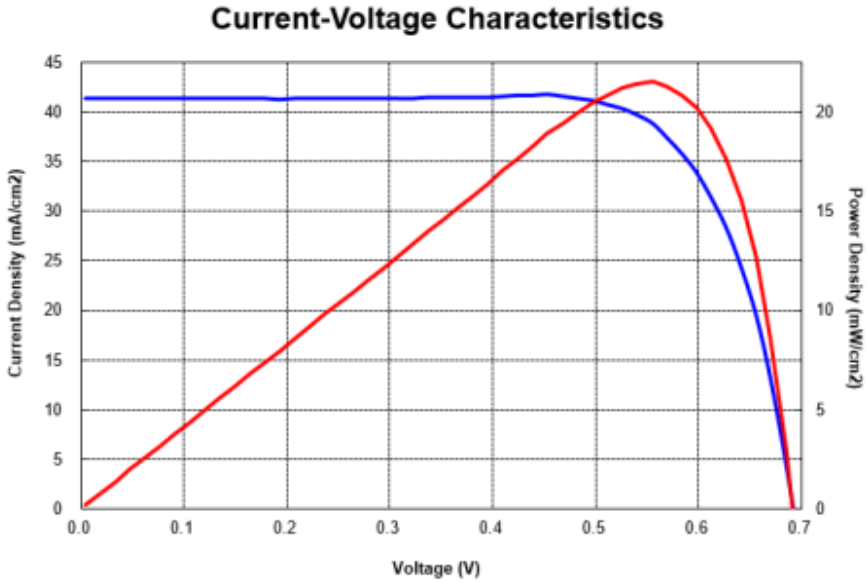

Figure 44: Current-voltage characteristics[25]

To maximize the power going into the energy storage a maximum power point tracking or mppt regulator is used to match the impedance of the circuit. This micro controller is seated between the output of the solar panel and energy storage.

To be able to use the capacitor as a energy storage for the thingy91 board the voltage must be regulated to 3.3V to power the nrf9160 SiP and 1.8V to power the GPIO and other peripherals

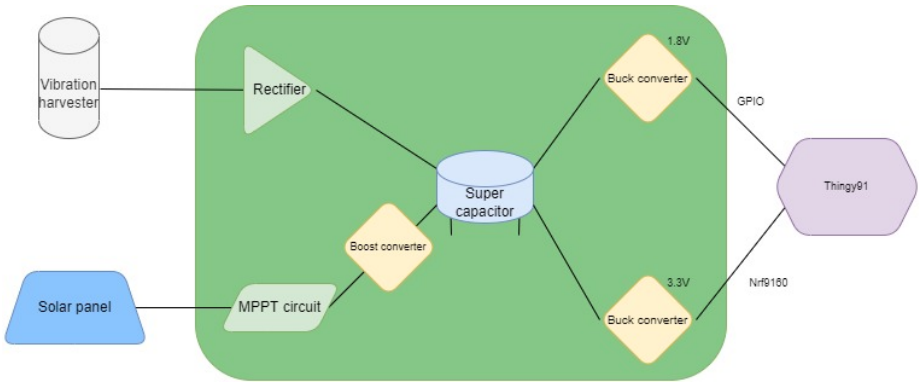

Figure 45: Solar panel and vibration harvester charging setup

6 Theory

To determine if the vibration energy and/or solar energy harvesting can support GNSS fix and LTE transmission, an understanding of the power consumption of the nrf9160 SiP and power output of the harvesters must be gathered.

6.1 Vibration energy harvester characteristics

To get an understanding of the VEH, a vibrator was connected to a sine wave generator. With this sine wave generator, vibrations of with different frequencies and accelerations could be produced.

The output of the VEH is connected to a 100 Ohm resistor as load. Over the resistance the voltage is measured with a oscilloscope and then analysed.

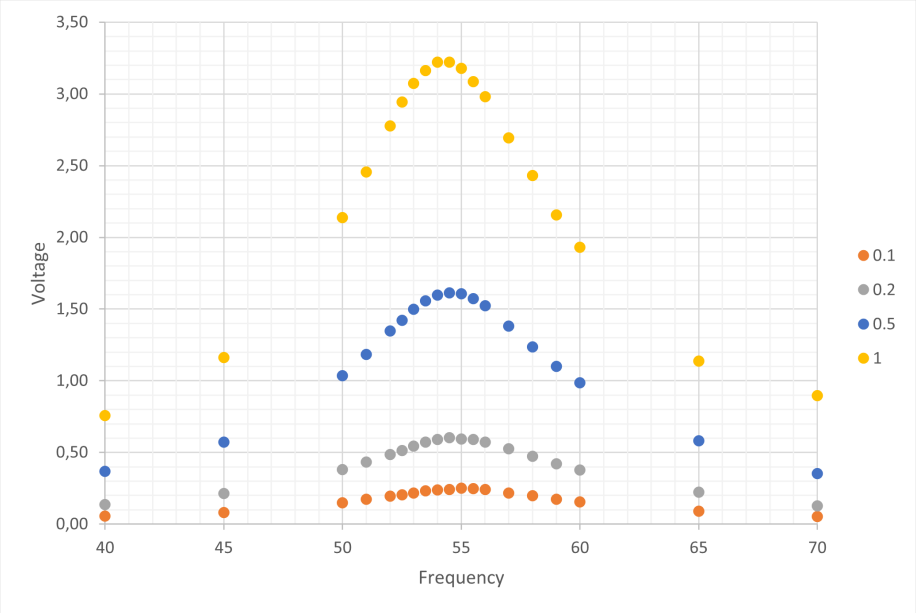

Figure 46: VEH peak to peak voltage output relative to frequency at different accelerations

In Figure 46 we can see that our vibration energy harvester is clearly tuned for 54 Hz with a quite steep voltage drop.

6.2 Shopping cart vibrations characteristics

The vibrating energy harvester will harvest the vibration energy created by a shopping cart. To understand the characteristics of the shopping cart the accelerometer on the thingy91 was setup to record the vibrations of the shopping cart.

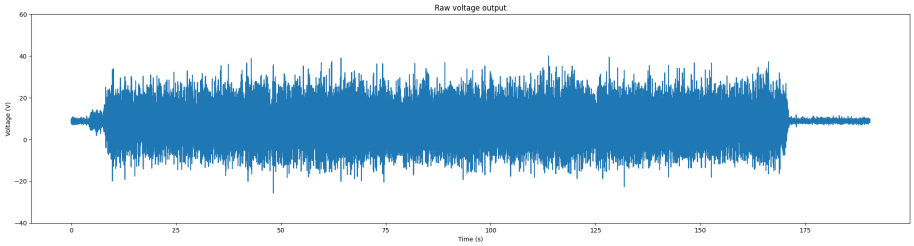

Figure 47: Raw voltage output of the accelerometer

To see if the shopping cart had a resonance frequency an accelerometer was set up and recorded the latitudinal vibrations at a sample rate of 200 Hz from which a frequency response analysis where made using fast Fourier transform.

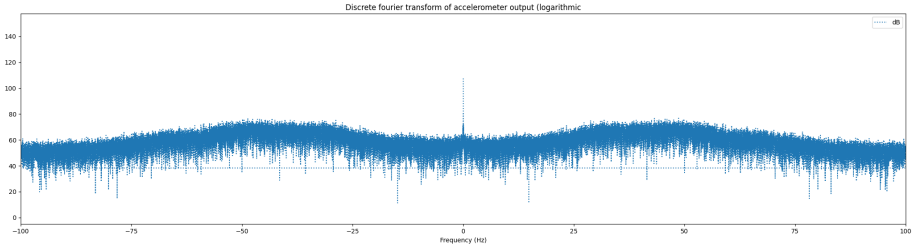

Figure 48: Fourier transform of the accelerometer raw output plotted logarithmically over time

There are not an obvious resonance frequency of the shopping cart vibrations when walking at "normal" walking speed. One can see a little hump between 25 an 75 Hz. To see how much of the vibration energy that will be harvested, the raw output from the accelerometer is filtered with a bandpass filter at the 50-60 Hz range, since this is the response frequency of our vibration energy harvester.

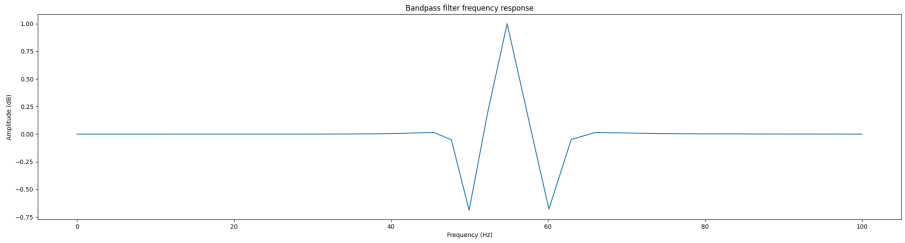

Figure 49: Bandpass filter response

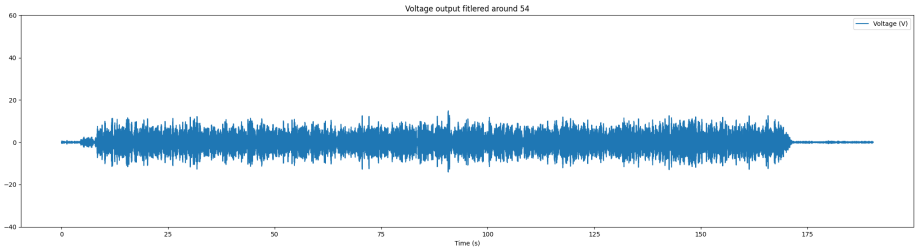

Figure 50: Filtered output from the accelerometer

As shown in Figure 50, the filtered accelerator output, which is a simple representation of the energy harvested by the harvester, is quite a bit lower compared to all vibrations made from the shopping cart.

6.3 Harvester output

The output of the vibration energy harvester was generated by mounting the harvester on a shopping cart and walking at "normal" walking speed over normal tarmac. The voltage was measured over a 1k Ohm resistor. The VEH is optimized for a frequency of 54 Hz.

6.3.1 Vibration energy harvester

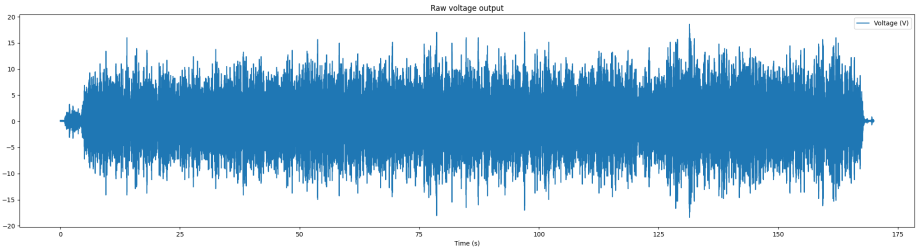

Figure 51: Raw voltage output with 1k Ohm resistance load plotted over time

Based on the raw voltage output and knowing the load, the power and energy output was calculated.

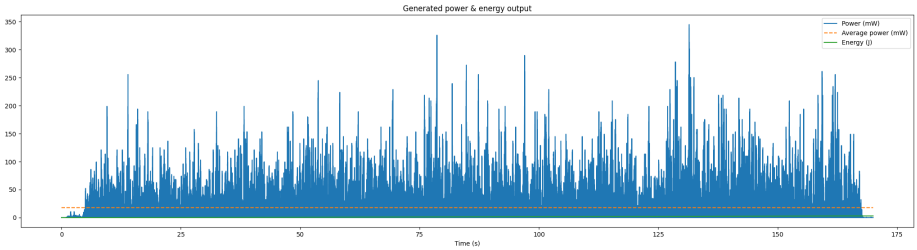

Figure 52: Power, average power & energy plotted against time

The current generated was calculated by dividing the raw voltage output by the resistance:

$$Current = \frac{Raw\ voltage\ output}{1k\ Ohm\ resistance}$$

The power generated was calculated by multiplying the raw output voltage with the calculated current:

$$Power = Raw\ voltage\ output * Current$$

The energy was calculated using the trapezoidal rule:

$$\int_a^b f(x)\,dx = \Big|F(b) - F(a)\Big|_a^b \approx \sum_{k=1}^{N} \frac{f(x_{k-1}) + f(x_k)}{2} * \Delta x_k \tag{1}$$

Rewrite 1 for calculating the energy output:

$$\sum_{i=1,2\ldots n}^{i} E_i = E_{i-1} + (P_i + P_{i-1}) * (T_i - T_{i-1}) \tag{2}$$

where E stands for energy, P for power, T for time and $E_0 = 0$

The average power generated was around 18mW during this 160 second interval. During this interval around 3 mJ of energy was produced.

6.3.2 Photovoltaic panel

The photovoltaic, or solar panel, used is a monocrystaline silicon solar panel called AnySolar KXOB121K04F [25]. The panel consists of four solar cells connected in series. The area of each cell is 121.475 mm^2. The power output of each cell is dependant of the irradiance the panel is exposed to accordingly.

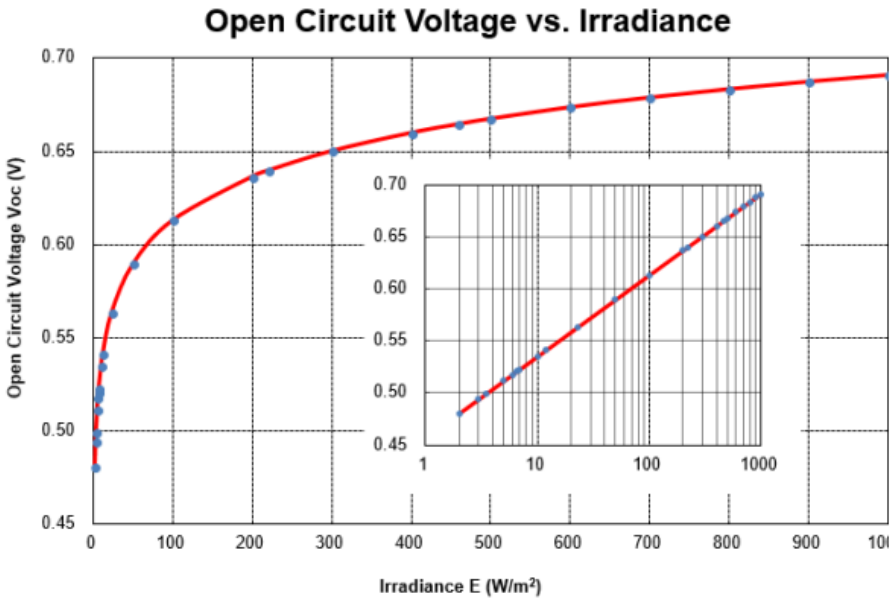

Figure 53: Open circuit voltage vs irradiance[25]

Irradiance is a measurement of the amount of absorbed light energy per area. Even though humans do not see that big of a difference between indoor and outdoor, the irradiance can vary a lot depending on the environment. The irradiance is directly correlated to the power output of any photovoltaic panel.

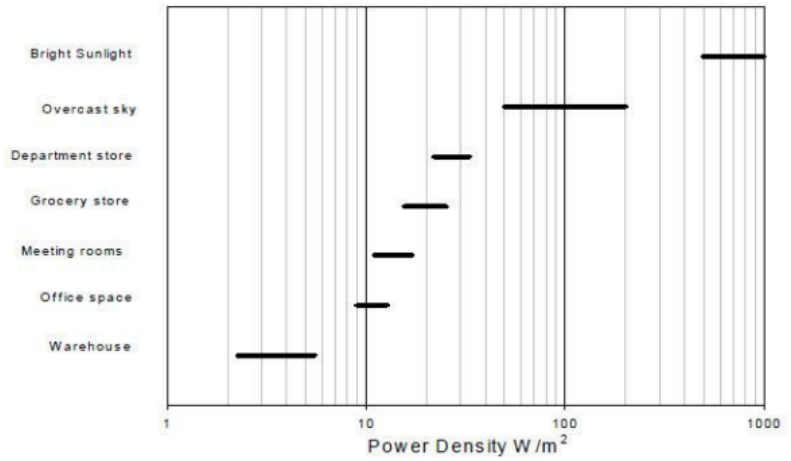

Figure 54: Power density/irradiance in different environments

According to the datasheet of the AnySolar KXOB121K04F the maximum power output is rated to 105.3 mW and is achieved at 1000 W/m^2. The rated conversion efficiency is 25%.

6.4 Theoretical model of GNSS fix and LPWAN transmission interval

A theoretical model is made from the gathered current measurements to understand how often the user equipment can gather GNSS fix and transmit data over LPWAN. The theoretical model describes the duration between a fix + transmission interval. The low power time described in the model is the time when the modem is in either PSM or eDRX.

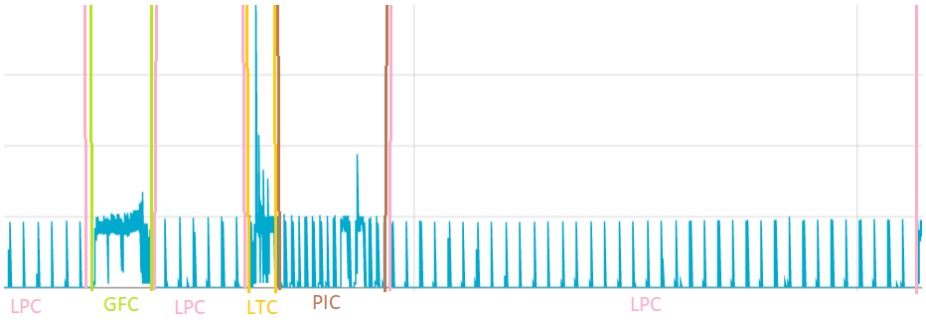

Figure 55: Current measurement of GNSS fix and LPWAN transmission example cycle

LPC = low power consumption, GFC = GNSS fix (acquisition) consumption, LTC = LTE transmission consumption, PIC = Paging interval consumption

$$I_{cc} = \frac{I_{GF} * T_{GF} + I_{LT} * T_{LT} + I_{PI} * T_{PI} + I_{LP} * T_{LP}}{T_{GF} + T_{LT} + T_{PI} + T_{LP}} \tag{3}$$

Where:
I_{cc} = Average charge current,
I_{GF} = GNSS fix current,
T_{GF} = GNSS fix time,
I_{LT} = LPWAN transmission current,
T_{LT} = LPWAN transmission time,
I_{PI} = Paging interval current,
T_{PI} = Paging interval time,
I_{LP} = Low power current,
T_{LP} = Low power time

The equation above is describing the average charging current when the low power time is just long enough to equalize the total consumption. Solve 3 for T_{LP} to find the low power time for an average charge current:

$$T_{LP} = \frac{-A_{PI} * T_{PI} - A_{GF} * T_{GF} - A_{LT} * T_{LT} + T_{GF} * I_{cc} + T_{LT} * I_{cc} + T_{PI} * I_{cc}}{A_{LP} - I_{cc}} \tag{4}$$

7 Technical choices

- Telia LTE-M & NB-IoT low power wide area networks - The only network available for this project at the time
- TCP and UDP protocols
- Thingy91 board
- ReVibe vibration energy harvester
- Anysolar KXOB121K04F photovoltaic harvester

Telia was chosen as an operator since that was the only SIM card obtainable at the moment. NB-IoT and LTE-M was the two investigated networks since they are specified by 3GPP where Ericsson is highly involved.

TCP and UDP protocols were the two chosen network protocols to test due to the low overhead they give and the reliability that TCP provides.

Thingy91 board was chosen since it contained all the features needed for the project and samples was available.

8 Software Implementation

Software was needed to be implemented both on the user equipment and in the cloud to get the application to work. The cloud was a necessity since sockets open to the internet is not allowed from the Ericsson internal network. Below is a figure describing the overall system architechture.

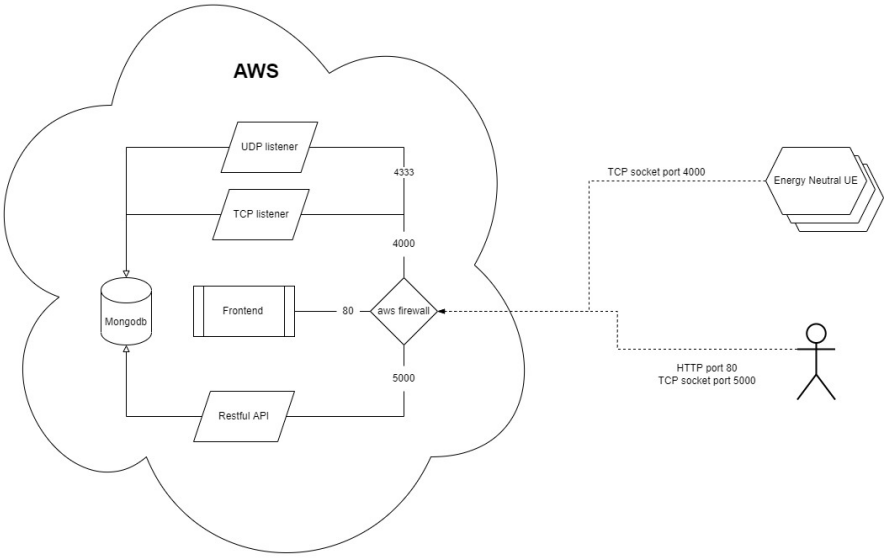

Figure 56: System overview

8.1 User equipment

To program the thingy91 we used C as the programming language, the real-time operating system *zephyr project* and the libraries *nrfxlib* and *nrf connect SDK*. When writing the code for the application, the standard of *MISRA-C (2012)* were followed. *MISRA-C (2012)* is a set of guidelines and rules that ensure safety, reliability and readability of the code. Example of these guidelines and rules are:

- Rule 9.1 (required) - All automatic variables shall have been assigned a value before being used. This rule is applied conservatively, meaning that if a variable may have been initialized prior to its first use, a diagnostic is not produced. The following is an example:

```
int x;

if (y == 0)
```

```
    x = 1;

x++; /* x is assumed to be initialized */
```

- Rule 19.2 (advisory) - Non-standard characters should not occur in header file names in #include directives.

Though the libraries did not always follow the guidelines. An assumption made were that these libraries are safe to use. To test the MISRA compliance the open source static analysis code checker *cppcheck* was used[10] together with a MISRA C (2012) addon built in Python.

The most important aspect of the software running on the user equipment is to make it as power efficient as possible. Since the most power consuming parts of the application is the LTE transmissions and the GNSS acquisitions, those are the most important things to optimize.

Before the GNSS is started, it is important to make sure that the modem is not used by the LTE, otherwise the GNSS would be on but would not get any data. When the GNSS is actively searching for a fix there is a concurrent GNSS event handler that handles incoming events such as Position, velocity and time (PVT) data. On a PVT data event, the code will examine the data and can stop executing at three conditions:

- Fix is available
- CN0 value is too low
- It has been searching for an excessive amount of time without getting a fix

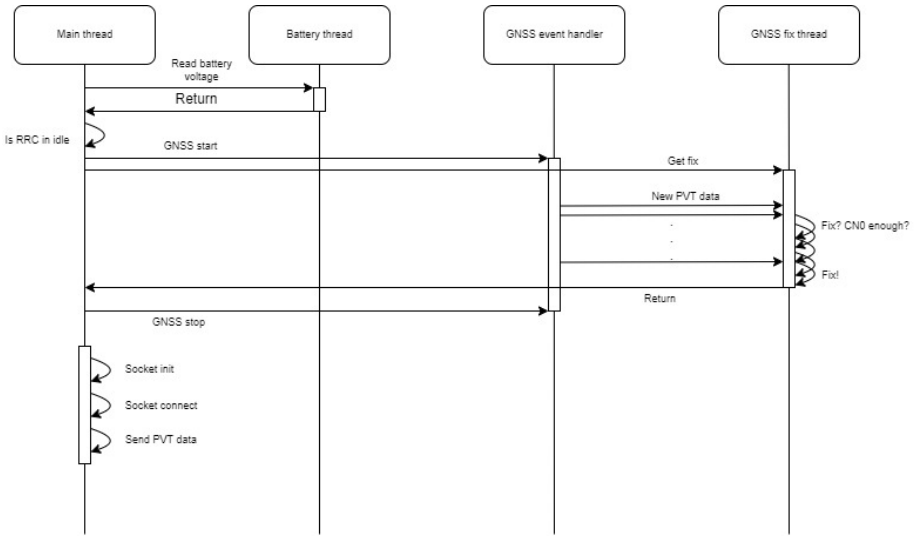

Figure 57: Sequence diagram of a typical 'get fix and transmit'

Since the application has multiple threads that share some variables and pointers, for example PVT data shared between GNSS event handler and GNSS fix thread as shown in Figure 57, thread safety must be ensured. This is done through using mutex locks when reading and writing to shared data.

8.2 Amazon web services - AWS

To visualize the geographical positions transmitted by the UE:s, a backend and frontend was built in an AWS EC2 instance. AWS EC2 is a virtual machine running Ubuntu in the AWS cloud. Using docker, four containers were created to build the backend system:

- TCP & UDP socket listeners
- MongoDB
- Restful api
- Frontend

The system architecture design is based upon microservices architecture. Microservices architecture is a system unlike a monolithic architecture built with multiple smaller services only being responsible for one area of the system. Microservice architecture was chosen because it improves separability, extendability and maintainability.

The socket listeners and the restful API are all implemented in python 3.4 since it is fast, easy to implement and works good with docker.

8.2.1 TCP and UDP socket listeners

The TCP and UDP socket listener is serving the UE:s. They receives the geographical data transmitted from the UE:s and inserts it into the mongo database.

8.2.2 MongoDB

The mongo database stores all geographical data sent from the UE:s. The database consists of one collection where each data point contains a longitude, a latitude, an accuracy and an id field. The data point is structered accordingly.

```
{
    "longitude": number,
    "latitude": number,
    "accuracy": number,
    "ID": number
}
```

The mongo database has not got any exposed ports to the internet but can only be accessed by other internal services.

8.2.3 Restful API

This http rest api have three endpoints. One to receive all data points, one to delete a specific locations and one to delete all data points made to reset a demo. Accordingly:

```
GET     "/locations"            - Get all location data-points
DELETE  "/locations"            - Delete all location data-points
DELETE  "/location/{location}   - Delete specific location data-point
```

The HTTP rest api is open to port 5000 to the network.

8.2.4 Frontend

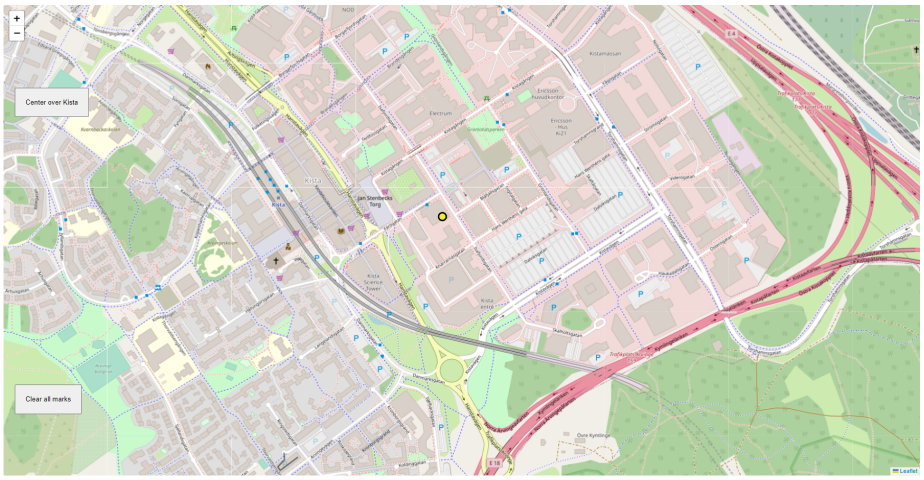

Figure 58: Frontend visualization

The frontend have one endpoint which returns html and javascript code which builds the frontend locally. The frontend makes http api calls to the rest api and uses *leaflet* to visualize the geographical data on the map. The frontend is open to the standard HTTP port 80.

9 Evaluation

9.1 Theoretical intervals with different average charging current

Since none of the current consumption measurements or the times of the current consumption measurements are constant, especially the GPS acquisition, an average was used from different measurements. Values used in the theoretical model:

- GNSS fix current: $I_{GF} = 41 * 10^{-3}\ A$
- GNSS fix time: $T_{GF} = 2.5s$
- LTE-M (TCP) transmission current: $I_{LT} = 22 * 10^{-3}\ A$
- LTE-M (TCP) transmission time: $T_{LT} = 6\ s$
- NB-IoT (UDP + RAI) transmission current: $I_{LT} = 22 * 10^{-3}\ A$
- NB-IoT (UDP + RAI) transmission time: $T_{LT} = 6\ s$
- Paging interval current: $I_{PI} = 3 * 10^{-3}\ A$
- Paging interval time: $T_{PI} = 6\ s$
- Power saving mode consumption: $I_{LP} = 3 * 10^{-6}\ A$
- Voltage = 5V

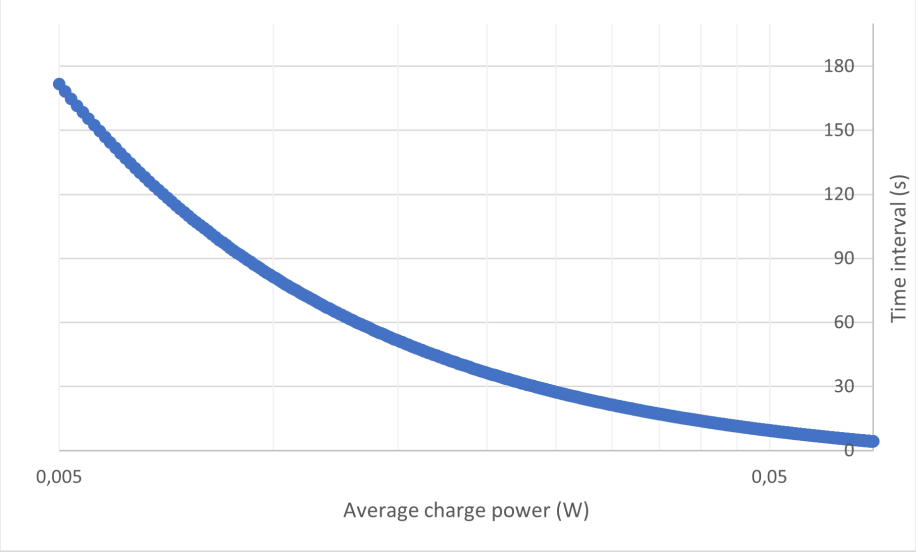

Figure 59: Theoretical time intervals possible at different average charging powers using LTE-M (TCP)

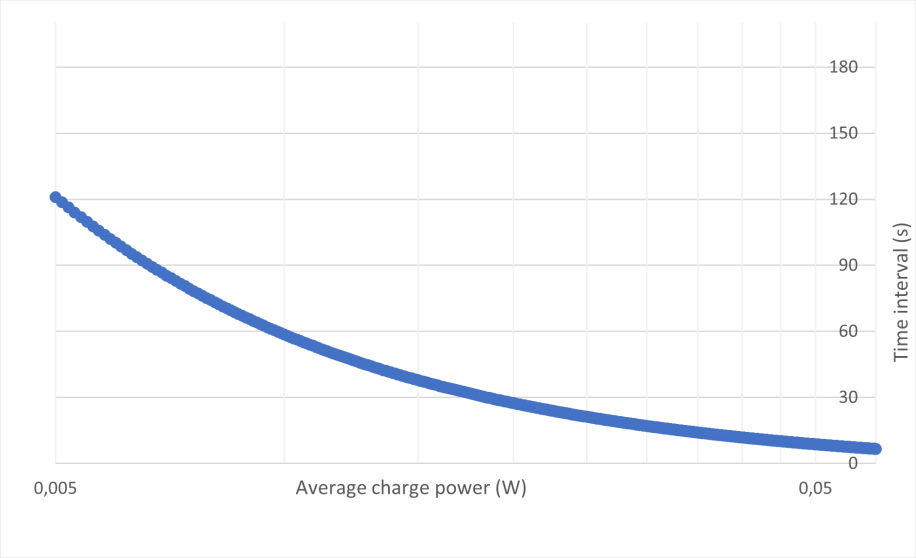

Figure 60: Theoretical time intervals possible at different average charging powers using NB-IoT (UDP + RAI)

9.2 Actual intervals

Gather results

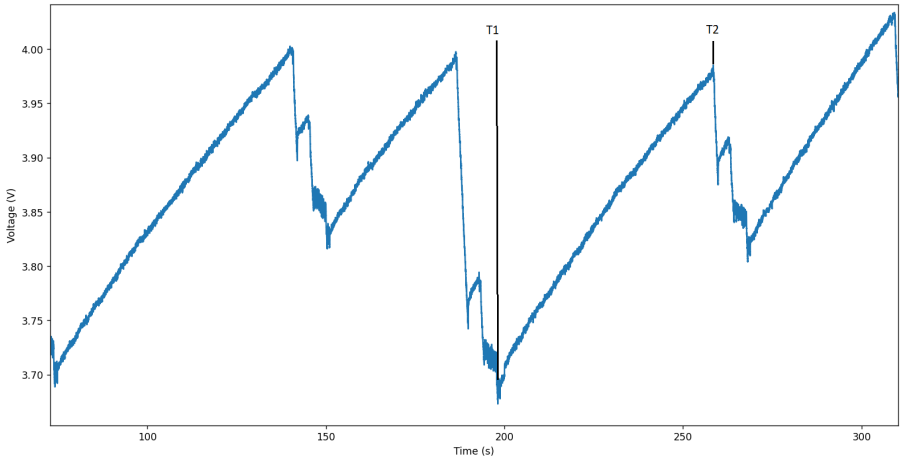

Figure 61: Example of power saving mode time measurement

To measure the intervals between a GPS fix and wireless transmission an oscilloscope was used to measure the voltage of the super-capacitor used, by marking

the beginning and the end of the power saving mode we get the time as the difference. The results gathered are the mean of multiple measurements.

Both energy harvesters used were tested under two different circumstances, optimal and sub optimal. The vibration energy harvester was tested by pushing a shopping cart at "normal" walking speed over a parking lot and a textured bike lane. The solar panel was tested in direct sunlight and in cloudy conditions. Two network conditions were also tested during the different circumstances: LTE-M using TCP and NB-IoT with RAI using UDP. In addition to the intervals the time it took for the GPS to acquire position data was also recognized since it has a large effect in the energy consumed between the fix and transmission intervals.

To get as big of a difference as possible on the measured voltage for visual and measuring purposes, as small of a capacitance on the super capacitor was used. While testing the application using LTE-M, a capacitor with the capacitance of 0.47F was used and while using the NB-IoT, a capacitor with the capacitance of 1F was needed. This was due to increased power consumption during the booting sequence of the application. During the booting sequence the application fetch GPS assistance data over the internet, since NB-IoT provides lower bandwidth compared to LTE-M this takes more time which results in higher energy consumption.

The amount of energy charging the super capacitor can be calculated by the following formula:

$$P = \frac{C * \frac{\sqrt{v_2}}{2} - C * \frac{\sqrt{v_1}}{2}}{t2 - t1} \tag{5}$$

where:
P = charging power,
C = capacitance of the supercapacitor,
v_2 = Measured voltage at time t_2,
v_1 = Measured voltage at time t_1

9.2.1 Vibration energy harvester on parking lot

While gathering energy from the vibration energy harvester while walking over a parking lot and having an average GPS acquisition time of about four seconds the average interval was measured to be around **65 seconds** while using LTE-M and TCP.

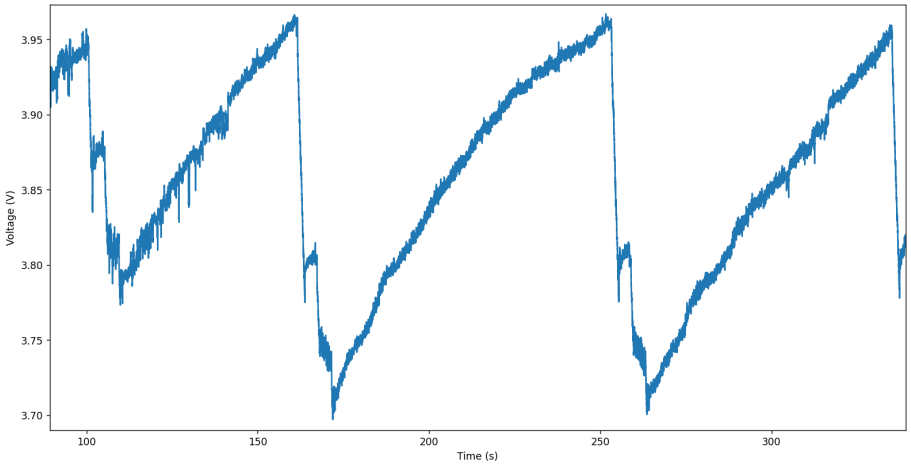

Figure 62: Voltage reading of the capacitor using LTE-M powered by the vibration energy harvester while walking on parking lot

While gathering energy from the vibration energy harvester while walking over a parking lot and having an average GPS acquisition time of about three seconds the average interval was measured to be around **27 seconds** while using NB-IoT and UDP with Release assistance indication.

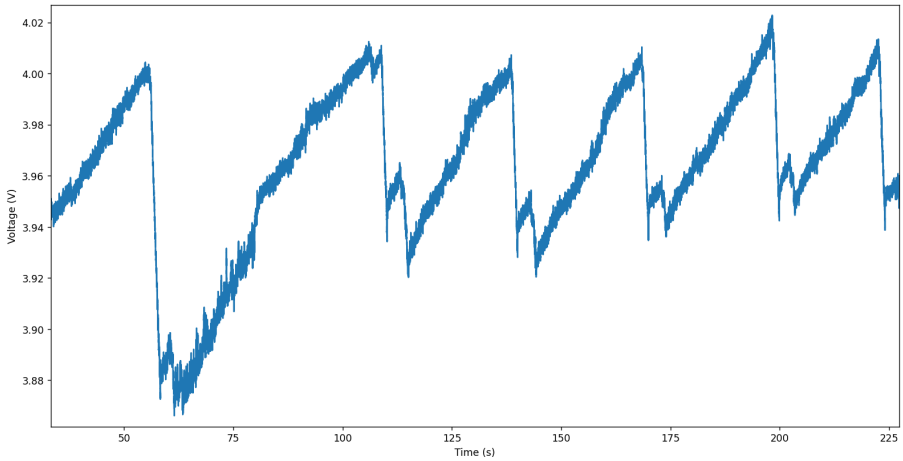

Figure 63: Voltage reading of the capacitor using NB-IoT powered by the vibration energy harvester while walking on parking lot

Using equation 5 and the voltage measurements an estimation of the power was calculated to be around 12 mW. According to the theoretical model that

amount of power would give us an interval of 48 seconds while using NB-IoT (UDP + RAI) and 66 seconds while using LTE-M (TCP).

9.2.2 Vibration energy harvester on textured bike lane

While gathering energy from the vibration energy harvester while walking over a textured bike lane and having a an average GPS acquisition time of about five seconds the average interval was measured to be around **64 seconds** while using LTE-M and TCP.

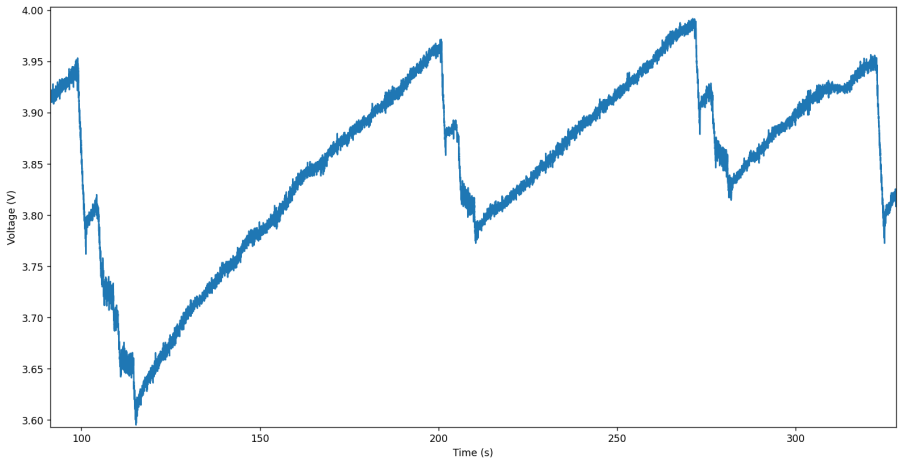

Figure 64: Voltage reading of the capacitor using LTE-M powered by the vibration energy harvester while walking on textured bike lane

While gathering energy from the vibration energy harvester while walking over a textured bike lane and having a an average GPS acquisition time of about two and a half seconds the average interval was measured to be around **23 seconds** while using NB-IoT and UDP with Release assistance indication.

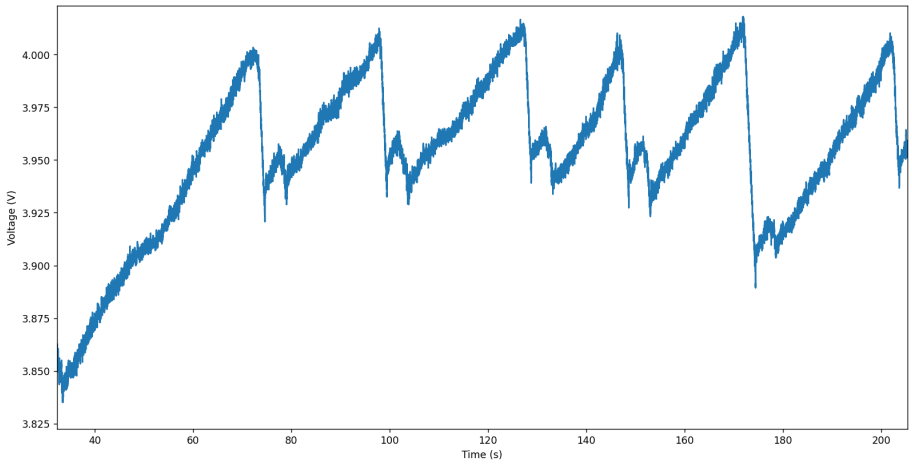

Figure 65: Voltage reading of the capacitor using NB-IoT powered by the vibration energy harvester while walking on textured bike lane

Using equation 5 and the voltage measurements an estimation of the power was calculated to be around 16 mW. According to the theoretical model that amount of power would give us an interval of 35 seconds while using NB-IoT (UDP + RAI) and 48 seconds while using LTE-M (TCP).

9.2.3 Photovoltaic panel during clear skies

While gathering energy from the photovoltaic panel during direct sunlight with an measured irradiance of around 500 W/m^2 and having a an average GPS acquisition time of about two and a half seconds the voltage increased during the tests which indicates we could do it continuously while using LTE-M and TCP.

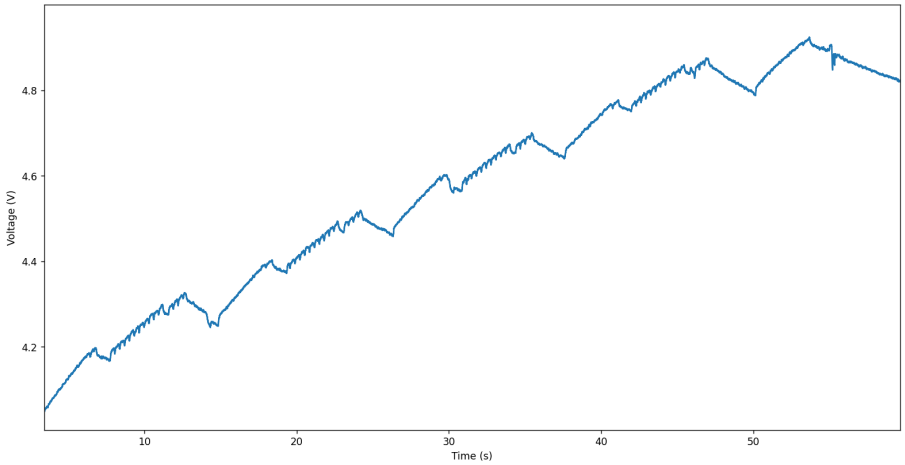

Figure 66: Voltage reading of the capacitor using LTE-M powered by the photovoltaic panel during clear skies

While gathering energy from the photovoltaic panel during direct sunlight with an measured irradiance of around 50 W/m^2 and having a an average GPS acquisition time of about three seconds the voltage increased during the tests which indicates we could do it continuously while using NB-IoT and UDP with Release assistance indication.

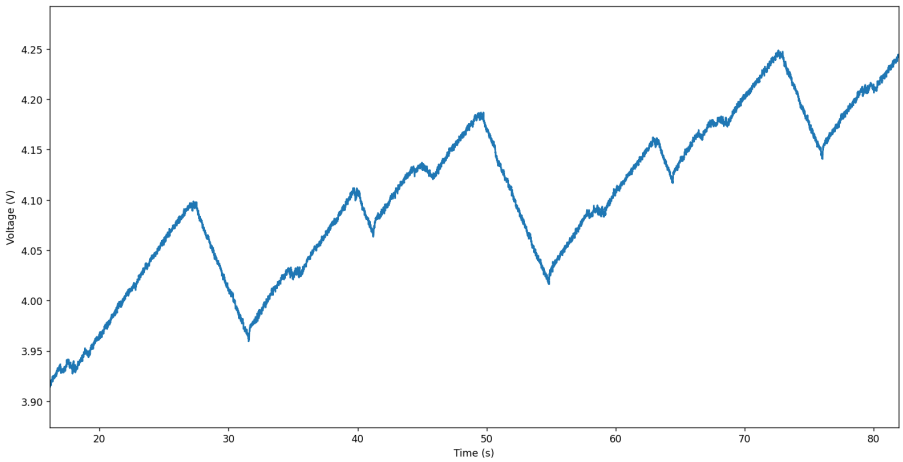

Figure 67: Voltage reading of the capacitor using NB-IoT powered by the photovoltaic panel during clear skies

Using equation 5 and the voltage measurements an estimation of the power was calculated to be around 90 mW. According to the theoretical model that

amount of power would give us an interval of three seconds while using NB-IoT (UDP + RAI) and one seconds while using LTE-M (TCP).

9.2.4 Photovoltaic panel during cloudy skies

While gathering energy from the photovoltaic panel during cloudy conditions with an measured irradiance of around 50 W/m^2 and having a an average GPS acquisition time of about 2.5 seconds the average intervals was measured to be around **46 seconds** while using LTE-M and TCP.

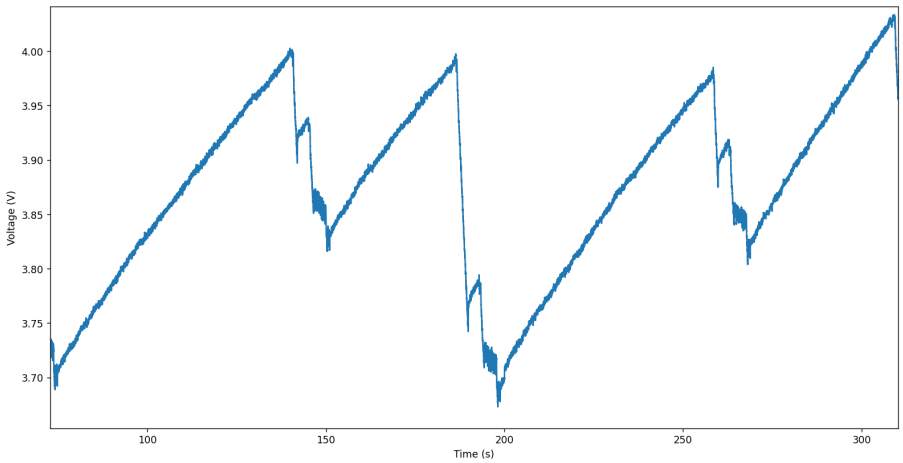

Figure 68: Voltage reading of the capacitor using LTE-M powered by the photovoltaic panel during cloudy skies

While gathering energy from the photovoltaic panel during cloudy conditions with an measured irradiance of around 50 W/m^2 and having a an average GPS acquisition time of about 2.5 seconds the average intervals was measured to be around **14 seconds** while using NB-IoT and UDP with Release assistance indication.

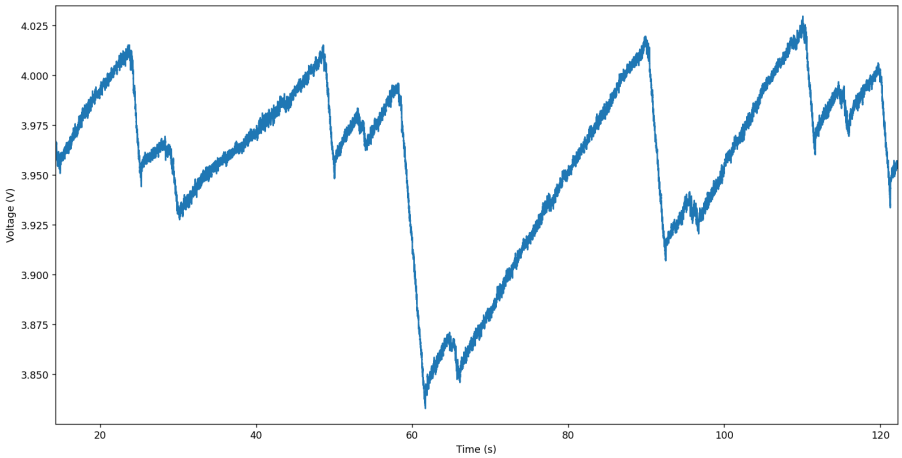

Figure 69: Voltage reading of the capacitor using LTE-M powered by the photovoltaic panel during cloudy skies

Using equation 5 and the voltage measurements, an estimation of the power was calculated to be around 20 mW. According to the theoretical model that amount of power would give us an interval of 27 seconds while using NB-IoT (UDP + RAI) and 36 seconds while using LTE-M (TCP).

9.2.5 Summary of actual intervals

Harvesters	Condition	Power (mW)	Network	Interval (s)
Vibration	Parking lot	12	LTE-M	65
			NB-IoT	27
	Bike lane	16	LTE-M	64
			NB-IoT	23
Photovoltaic	Clear skies	90	LTE-M	$\sim$
			NB-IoT	$\sim$
	Cloudy	20	LTE-M	46
			NB-IoT	14

10 Discussion

The idea of this project was to see if we could gather enough energy using small energy harvesters mounted on a shopping cart to acquire GNSS position and send it over LPWAN. The answer to this question is not obvious since there are a lot of factors affecting both the power consumption of the application and the charging output of the harvesters that cannot be handled, such as the environmental effects on the GNSS acquisition, the environmental effect on the charging output and the network timers regulated by the operators.

Telia unwanted traffic

The first SIM card used was a Telia SIM card that connected to LTE-M and NB-IoT. Using this SIM a lot of random incoming traffic was recorded during the paging interval. Incoming messages during the paging window prevents the modem to sleep which in turn consumes power.

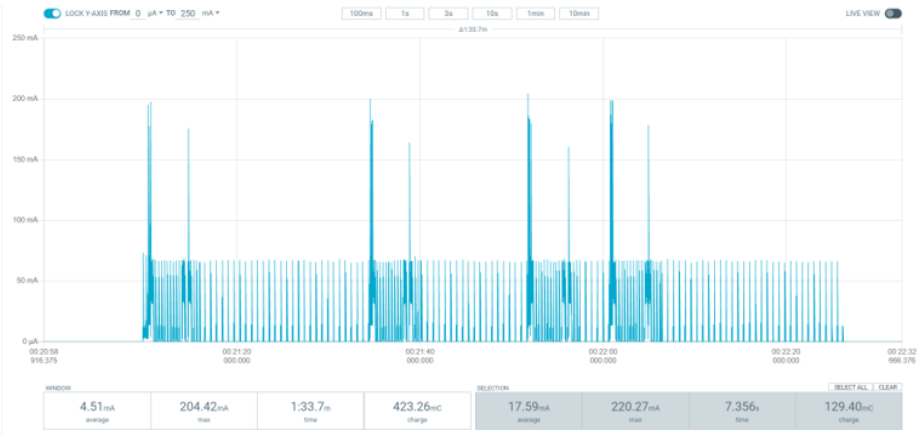

Figure 70: Traffic resetting the modems paging interval

Luckily the solution to this problem was to switch the SIM card to a dedicated Telia IoT SIM card. One could request to not having a paging interval at all but since this is regulated by the operator this was not a reliable solution.

GNSS power consumption

When testing the current consumption of the GNSS part of the application it was tested with the nrf9160dk which has a dedicated antenna for the GNSS. When the code was compiled and tested for the thingy91 the GNSS took a lot longer time to acquire a fix. This is due to the thingy91 only having one antenna shared between the LTE and GNSS. This antenna is optimized for LTE communications. To solve this issue an external antenna optimized for GPS is

used. Even though the external antenna is optimized for GPS the acquisition time can very a lot depending on the environment such as cloud and buildings etc.

Reception impact

The transmission power while using both LTE-M and NB-IoT is regulated dynamically depending on the current reception signal of the modem. While testing this device the test area was restricted to how far one could walk with the shopping cart which was fairly restricted. This should be further investigated to get an understanding of how large effect it will have on the overall power consumption.

Transmission size

In the tests, we got shorter intervals while using NB-IoT with release assistance indication and using UDP protocol. However, because of the lower bandwidth of NB-IoT compared to LTE-M this could be due tp the small size of our transmissions. For use cases that requires to transmit more data an LTE-M transmission might be more energy efficient. This was observed while measuring the voltage of the super capacitor while retrieving GPS assistance data but the exact breaking point cannot be determined in this thesis.

Altercations to the cart

The small frequency response of the vibration energy harvester and the lack of a resonance in the frequency of the shopping cart while walking on tarmac was a big issue in the power output of the harvester. To resolve this, an idea was to create shopping cart wheels with the shape of an pentagon or hexagon to increase the vibrations at a specific frequency while walking with a certain speed. This was unfortunately not made due to time restrictions. Another alternative to solve this problem would be to completely discard the vibration harvester and instead use a hub generator, harvesting the kinetic energy of the wheel rolling.

Base-station switching during NB-IoT

Even though NB-IoT was shown to be more power efficient in this use case there were some problems detected using NB-IoT. During testing the modem would switch base-stations at random causing the application to be put on hold and also consuming a lot of power since NB-IoT requires a new network registration every time it switches base-station. This could be an issue if deployed in an area in the middle of two base-stations. This was not experienced while using LTE-M network.

11 Conclusion

In this study two questions were investigated:

1. Is it possible to harvest enough energy using a small energy harvester mounted on a shopping cart to power a thingy91 to get a geographical position and send it over a low power wide area network?

2. How often is it possible to get geographical position and transmit over low power wide area networks using harvested energy?

Regarding the first question the answer is yes as long as the shopping cart is either moving over a rough surface or if it is exposed to an irradiance of at least 50 W/m^2. The second question is harder to specify, in optimal conditions the device can gather geographical position and transmit over both LTE-M and NB-IoT continuously, while in the worst conditions it would never be able to transmit its position. It is very much dependant on several factors which all have not been tested.

Comparing the values gotten from the theoretical model and the real world measurements it seems like the consumption and charging power is too unpredictable to calculate accurately, at best it can provide an rough estimation. In addition there are factors not taken into account such as efficiency of the power management board.

11.1 Future work

The subject of this project is a big research area and there are a lot of work that could be done to improve the results of this project.

Vibration energy harvesters are being researched to provide a wider frequency response which in this use cases, such as this project, would benefit the power output vastly.

Instead of using only a rectifier between the vibration energy harvester and the energy storage, a power management that could impedance match the unstable and irregular voltage output of the harvester itself would also make a vibration energy harvester more applicable under more circumstances.

Ericsson themselves are continuously investigating ways to further lower the power consumption of wide area networks which improvement would greatly impact the use of LPWAN:s in more and more IoT devices with more and more demanding applications.

Antenna improvement and efficiency would also result in lower power consumption both by the LTE-M consuming less power while both transmitting and receiving and by the GPS where a superior antenna could potentially lower the

GPS fix acquisition time both in good and bad weather conditions.

In this project the application only transmitted data and never had to listen or retrieve any down-link communication. This would be an interesting project to conduct to figure out if it is possible to use energy harvested by small energy harvester to power such an application continuously.

References

[1] *230 EDLC-HV ENYCAP*. URL: https://eu.mouser.com/datasheet/2/427/VISH_S_A0011831053_1-2572302.pdf. (accessed: 30.08.2022).

[2] *AAA uppladdningsbar 1,6 V 900 mWh NIZN*. URL: https://www.amazon.se/PKCELL-uppladdningsbart-batteri-leksakskamera-pannlampa/dp/B01DEUMO4W/ref=asc_df_B01DEUMO4W/?tag=shpngadsglede-21&linkCode=df0&hvadid=476491192222&hvpos=&hvnetw=g&hvrand=9378900247954134213&hvpone=&hvptwo=&hvqmt=&hvdev=c&hvdvcmdl=&hvlocint=&hvlocphy=9062465&hvtargid=pla-586067410497&psc=1. (accessed: 30.08.2022).

[3] *ACL9012 -3.3Ah*. URL: https://docs.rs-online.com/f092/0900766b812fdd0f.pdf. (accessed: 30.08.2022).

[4] *ACL9013*. URL: https://docs.rs-online.com/4ad1/0900766b812fdd10.pdf. (accessed: 30.08.2022).

[5] "Chapter 7 - High Efficiency Plants and Building Integrated Renewable Energy Systems". In: *Handbook of Energy Efficiency in Buildings*. Ed. by Francesco Asdrubali and Umberto Desideri. Butterworth-Heinemann, 2019, pp. 441–595. ISBN: 978-0-12-812817-6. DOI: https://doi.org/10.1016/B978-0-12-812817-6.00040-1. URL: https://www.sciencedirect.com/science/article/pii/B9780128128176000401. (accessed: 30.08.2022).

[6] *Assisted GNSS (AssistNow)*. 2020. URL: https://www.u-blox.com/en/technologies/agnss-assistnow. (accessed: 30.08.2022).

[7] *BK-26SCSA01*. URL: https://www.mouser.se/datasheet/2/315/panasonic_04112018_BK-26SCSA01-01-01-1317129.pdf. (accessed: 30.08.2022).

[8] Mark Bloechl. "LTE eDRX and PSM Explained for LTE-M1". In: (2016). URL: https://www.link-labs.com/blog/lte-e-drx-psm-explained-for-lte-m1. (accessed: 30.08.2022).

[9] Matteo Cossutta et al. "A comparative life cycle assessment of graphene and activated carbon in a supercapacitor application". In: *Journal of Cleaner Production* 242 (2020), p. 118468. ISSN: 0959-6526. DOI: https://doi.org/10.1016/j.jclepro.2019.118468. URL: https://www.sciencedirect.com/science/article/pii/S0959652619333384. (accessed: 30.08.2022).

[10] *Cppcheck website*. URL: http://cppcheck.net/. (accessed: 30.08.2022).

[11] *DX1500*. URL: https://docs.rs-online.com/f209/0900766b814eb1d3.pdf. (accessed: 30.08.2022).

[12] Hassan Elahi, Marco Eugeni, and Paolo Gaudenzi. *Chapter 3 - Energy harvesting*. Ed. by Hassan Elahi, Marco Eugeni, and Paolo Gaudenzi. 2022. DOI: https://doi.org/10.1016/B978-0-12-823968-1.00014-3. URL: https://www.sciencedirect.com/science/article/pii/B9780128239681000143. (accessed: 30.08.2022).

[13] Diana Enescu. "Thermoelectric Energy Harvesting: Basic Principles and Applications". In: *Green Energy Advances*. Ed. by Diana Enescu. Rijeka: IntechOpen, 2019. Chap. 1. DOI: 10.5772/intechopen.83495. URL: https://doi.org/10.5772/intechopen.83495. (accessed: 30.08.2022).

[14] Pamela Fox. *Transmission Control Protocol (TCP)*. URL: https://www.khanacademy.org/computing/computers-and-internet/xcae6f4a7ff015e7d:the-internet/xcae6f4a7ff015e7d:transporting-packets/a/transmission-control-protocol--tcp. (accessed: 30.08.2022).

[15] Pamela Fox. *User Datagram Protocol (UDP)*. URL: https://www.khanacademy.org/computing/computers-and-internet/xcae6f4a7ff015e7d:the-internet/xcae6f4a7ff015e7d:transporting-packets/a/user-datagram-protocol-udp. (accessed: 30.08.2022).

[16] Carsten Rhod Gregersen. *The basics of IoT's Constrained Application Protocol (CoAP)*. 2021. URL: https://www.embedded.com/the-basics-of-iots-constrained-application-protocol-coap/. (accessed: 30.08.2022).

[17] Joel Höglund et al. "PKI4IoT: Towards Public Key Infrastructure for the Internet of Things". In: *Computers & Security* 89 (Nov. 2019). DOI: 10.1016/j.cose.2019.101658. (accessed: 30.08.2022).

[18] *HR06*. URL: https://www.conrad.se/p/conrad-energy-hr06-laddbart-batteri-aa-r6-nizn-1500-mah-16-v-4-st-252000. (accessed: 30.08.2022).

[19] *ICP501233PA*. URL: https://www.elfa.se/Web/Downloads/_t/ds/ICP501233PA_eng_tds.pdf. (accessed: 30.08.2022).

[20] *INR18650-25R*. URL: https://cdn.shopify.com/s/files/1/0481/9678/0183/files/samsung_25r_data_sheet.pdf?v=1605015771. (accessed: 30.08.2022).

[21] *INR18650-30Q*. URL: https://cdn.shopify.com/s/files/1/0481/9678/0183/files/samsung_30q_data_sheet.pdf. (accessed: 30.08.2022).

[22] *INR18650-35E*. URL: https://cdn.shopify.com/s/files/1/0481/9678/0183/files/samsung_35e_data_sheet.pdf?v=1605015771. (accessed: 30.08.2022).

[23] *INR18650/33V*. URL: https://cdn.shopify.com/s/files/1/0481/9678/0183/files/EVE_INR18650-33V_RD-EVE_INR18650-33V-S88-LF-A.pdf?v=1633373306. (accessed: 30.08.2022).

[24] Dali Ismail, Mahbubur Rahman, and Abusayeed Saifullah. *Low-power wide-area networks: opportunities, challenges, and directions*. Jan. 2018. DOI: 10.1145/3170521.3170529. (accessed: 30.08.2022).

[25] *IXOLARTM High Efficiency SolarMD*. URL: https://waf-e.dubudisk.com/anysolar.dubuplus.com/techsupport@anysolar.biz/O18AzS1/DubuDisk/www/Gen3/KXOB121K04F%5C%20DATA%5C%20SHEET%5C%2020210127.pdf. (accessed: 30.08.2022).

[26] Angelo Joseph and Mark Petovello. *Measuring GNSS signal strength*. 2010. URL: https://insidegnss.com/wp-content/uploads/2018/01/novdec10-Solutions.pdf. (accessed: 30.08.2022).

[27] Jarod Kelly, Qiang Dai, and Michael Wang. "Globally regional life cycle analysis of automotive lithium-ion nickel manganese cobalt batteries". In: *Mitigation and Adaptation Strategies for Global Change* 25 (Mar. 2020). DOI: 10.1007/s11027-019-09869-2. (accessed: 27.10.2022).

[28] Emily Mcmilin. "Ambient RF energy Harvesting". In: (2014). URL: http://large.stanford.edu/courses/2014/ph240/mcmilin2/. (accessed: 30.08.2022).

[29] Kais Mekki et al. "A comparative study of LPWAN technologies for large-scale IoT deployment". In: *ICT Express* 5.1 (2019), pp. 1–7. ISSN: 2405-9595. DOI: https://doi.org/10.1016/j.icte.2017.12.005. URL: https://www.sciencedirect.com/science/article/pii/S2405959517302953. (accessed: 30.08.2022).

[30] *Miniature thermoelectric generators*. URL: https://www.tec-microsystems.com/products/thermoelectric-generators/index.html. (accessed: 30.08.2022).

[31] *MQTT*. URL: https://mqtt.org/. (accessed: 30.08.2022).

[32] *NB-IoT, LoRaWAN, Sigfox: An up-to-date comparison*. URL: https://iot.telekom.com/resource/blob/data/492968/e396f72b831b0602724ef71056af5045/mobile-iot-network-comparison-nb-iot-lorawan-sigfox.pdf. (accessed: 30.08.2022).

[33] *Nowi Powered Energy Autonomous Nordic Thingy:91 Platform*. URL: https://devzone.nordicsemi.com/nordic/nordic-blog/b/blog/posts/nowi-powered-energy-autonomous-nordic-thingy-91-platform. (accessed: 30.08.2022).

[34] Ermanno Pietrosemoli. *Wireless standards for IoT: WiFi, BLE, SigFox, NB-IoT and LoRa*. 2017. URL: http://wireless.ictp.it/school_2017/Slides/IoTWirelessStandards.pdf. (accessed: 30.08.2022).

[35] *Red Power RC Batteripack (LiPo) 3.7 V 800 mAh Antal celler: 1 25 C Softcase BEC*. URL: https://www.conrad.se/p/red-power-rc-batteripack-lipo-37-v-800-mah-antal-celler-1-25-c-softcase-bec-1890528. (accessed: 30.08.2022).

[36] Institute for energy research. "The Environmental Impact of Lithium Batteries". In: (2020). URL: https://www.instituteforenergyresearch.org/renewable/the-environmental-impact-of-lithium-batteries/. (accessed: 30.08.2022).

[37] *RS PRO Supercapacitor*. URL: https://docs.rs-online.com/1561/0900766b8170addc.pdf. (accessed: 30.08.2022).

[38] *RS PRO, 1.2V, 18670, NiMH Rechargeable Battery, 4Ah*. URL: https://uk.rs-online.com/web/p/speciality-size-rechargeable-batteries/9175923. (accessed: 30.08.2022).

[39] *RSAML9131*. URL: https://docs.rs-online.com/c8bb/0900766b8172be40.pdf. (accessed: 30.08.2022).

[40] Vasil Sarafov and Jan Seeger. "Comparison of IoT Data Protocol Overhead". In: (2018). URL: https://www.net.in.tum.de/fileadmin/TUM/NET/NET-2018-03-1/NET-2018-03-1_02.pdf. (accessed: 30.08.2022).

[41] Noureen Siraj et al. "Metal-Free Carbon-Based Supercapacitors—A Comprehensive Review". In: *Electrochem* 1.4 (2020), pp. 410–438. ISSN: 2673-3293. DOI: 10.3390/electrochem1040028. URL: https://www.mdpi.com/2673-3293/1/4/28. (accessed: 30.08.2022).

[42] *SR674361P*. URL: https://www.mouser.com/datasheet/2/272/SR674361P_RevB_-_Updated_datasheet-1272922.pdf. (accessed: 30.08.2022).

[43] Patrik Starck. "Energy harvesting of ambient radio waves". In: (2018). ISSN: 1401-5757. URL: https://uu.diva-portal.org/smash/get/diva2:1223582/FULLTEXT01.pdf. (accessed: 30.08.2022).

[44] International committee on global navigation satellite systems. *GNSS, How it Works and Applications*. 2018. URL: https://www.unoosa.org/documents/pdf/psa/activities/2018/ArgentinaGNSS/IDM_Seminar/D1-02.pdf. (accessed: 30.08.2022).

[45] *Telia LPWAN network coverage*. URL: https://www.telia.se/privat/support/tackningskartor#/tckningskartafrmobiltelefonimobilsurf. (accessed: 30.08.2022).

[46] Oskar Thorin. "Power Line Induction Energy Harvesting Powering Small Sensor Nodes". In: (2016). ISSN: DiVA, id: diva2:931356. URL: https://www.diva-portal.org/smash/get/diva2:931356/FULLTEXT01.pdf. (accessed: 30.08.2022).

[47] Mohammed Usman. *Industry adoption of IoT: a constrained application protocol survey*. 2014. URL: https://www.embedded.com/industry-adoption-of-iot-a-constrained-application-protocol-survey/. (accessed: 30.08.2022).

[48] *Voltaic panel*. URL: https://voltaicsystems.com/0-6-watt-6-volt-solar-panel-etfe/. (accessed: 27.10.2022).

[49] Chongfeng Wei and Xingjian Jing. "A comprehensive review on vibration energy harvesting: Modelling and realization". In: *Renewable and Sustainable Energy Reviews* 74 (2017), pp. 1–18. ISSN: 1364-0321. DOI: https://doi.org/10.1016/j.rser.2017.01.073. URL: https://www.sciencedirect.com/science/article/pii/S1364032117300837. (accessed: 30.08.2022).

[50] *What are LoRa® and LoRaWAN®?* URL: https://lora-developers.semtech.com/documentation/tech-papers-and-guides/lora-and-lorawan/. (accessed: 30.08.2022).

[51] Evelina Wikner. "Lithium ion Battery Aging: Battery Lifetime Testing and Physics-based Modeling for Electric Vehicle Applications". In: (2017). URL: https://publications.lib.chalmers.se/records/fulltext/249356/249356.pdf. (accessed: 30.08.2022).